molecular pharmaceutics

articles

Amide−*N*-Oxide Heterosynthon and Amide Dimer Homosynthon in Cocrystals of Carboxamide Drugs and Pyridine *N*-Oxides

N. Jagadeesh Babu, L. Sreenivas Reddy, and Ashwini Nangia*

School of Chemistry, University of Hyderabad, Hyderabad 500 046, India

Received January 23, 2007; Revised Manuscript Received March 27, 2007; Accepted April 6, 2007

Abstract: The carboxamide−pyridine *N*-oxide heterosynthon is sustained by *syn*(amide)-N−H···O⁻(oxide) hydrogen bond and auxiliary (*N*-oxide)C−H···O(amide) interaction (Reddy, L. S.; Babu, N. J.; Nangia, A. *Chem. Commun.* **2006**, 1369). We evaluate the scope and utility of this heterosynthon in amide-containing molecules and drugs (active pharmaceutical ingredients, APIs) with pyridine *N*-oxide cocrystal former molecules (CCFs). Out of 10 cocrystals in this study and 7 complexes from previous work, amide−*N*-oxide heterosynthon is present in 12 structures and amide dimer homosynthon occurs in 5 structures. The amide dimer is favored over amide−*N*-oxide synthon in cocrystals when there is competition from another H-bonding functional group, e.g., 4-hydroxybenzamide, or because of steric factors, as in carbamazepine API. The molecular organization in carbamazepine·quinoxaline *N*,*N*′-dioxide 1:1 cocrystal structure is directed by amide homodimer and *anti*(amide)N−H···O⁻(oxide) hydrogen bond. Its X-ray crystal structure matches with the third lowest energy frame calculated in Polymorph Predictor (Cerius^2, COMPASS force field). Apart from generating new and diverse supramolecular structures, hydration is controlled in one substance. 4-Picoline *N*-oxide deliquesces within a day, but its cocrystal with barbital does not absorb moisture at 50% RH and 30 °C up to four weeks. Amide−*N*-oxide heterosynthon has potential utility in both amide and *N*-oxide type drug molecules with complementary CCFs. Its occurrence probability in the Cambridge Structural Database is 87% among 27 structures without competing acceptors and 78% in 41 structures containing OH, NH, H_2O functional groups.

Keywords: Homosynthon; heterosynthon; carboxamide; pyridine *N*-oxide; pharmaceutical; cocrystal

Introduction

Chemical crystallographers have studied molecular complexes and molecular compounds for over a century.[1] There is a resurgence of interest in multi-component solid-state assemblies[2] under the banner of a new name, cocrystal.[3] The generally accepted definition of cocrystal is a crystalline adduct between two neutral molecules that are solids at ambient conditions and held together by hydrogen bonds in the complex.[4] We propose that the definition of cocrystal be expanded to accommodate solvent (liquid) or gas as the second (third) component and the supramolecular interaction be not limited to hydrogen bonds but also include other intermolecular interactions, such as halogen bonds,[5] $\pi-\pi$ stacking,[6] and ion pairing.[7] In a broad sense, the term cocrystal should encompass all multi-component solid-state assemblies of two or more molecules held together by any type or combination of intermolecular interactions.[8] Cocrystals not only exhibit structural novelty and supramolecular diversity, they are important in pharmaceutical

* Author to whom correspondence should be addressed. Mailing address: Department of Chemistry, University of Hyderabad, Hyderabad 500 046, India. E-mail: ashwini_nangia@rediffmail.com. Tel: +91 40 2301 1338. Fax: +91 40 2301 1338.

(1) (a) Kitaigorodskii, A. I. *Mixed Crystals*; Springer: Berlin, 1984; pp 275−318. (b) Herbstein, F. H. *Crystalline Molecular Complexes and Compounds*; IUCr Monographs, Vols. 1−2; Oxford University Press: Oxford, 2005.

10.1021/mp070014c CCC: $37.00
Published on Web 05/12/2007

formulation for producing new, improved medicines.[9] Attempted co-crystallization led to the serendipitous discovery of novel polymorphs of several common compounds: aspirin, maleic acid, benzidine, and oxalyl dihydrazide.[10] Pharmaceutical cocrystals are hydrogen-bonded complexes between an active pharmaceutical ingredient (API) and another solid component,[4a,9a] the second species usually being a benign excipient, a different drug molecule, or a solubilizing agent. Pharmaceutical cocrystals offer potential benefits of superior efficacy, solubility, and stability in drug formulation. Quite apart from their scientific curiosity and pharmaceutical application, the meaning and writing style of the word cocrystal (or co-crystal) was debated.[3] We consistently use the term cocrystal (without hyphen) for a chemical reason. The molecular components are distinct chemical entities prior to crystallization, and so using the hyphen in co-crystallization is appropriate because co- implies bringing two different molecules together. However,

Scheme 1. Strong Hydrogen Bond Homosynthons and Acid−Pyridine Heterosynthon with Their Occurrence Probability Indicated[a]

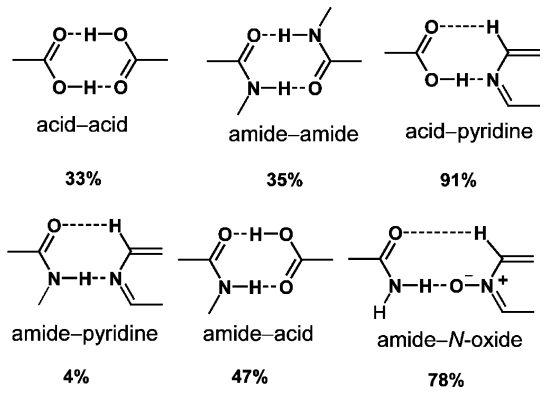

[a] Amide *N*-oxide frequency is estimated in this study. Other values are taken from refs 12 and 13.

Scheme 2. Hydrogen Bond Synthon Energy of Amide−*N*-Oxide Heterosynthon Calculated in Spartan 04 (HF/6-31G**)[a]

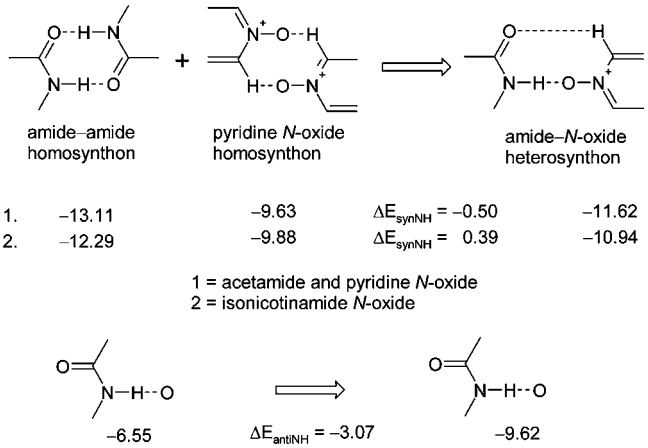

[a] The net stabilization in heterosynthon compared to homosynthons, ΔE_{HB}, is ∼3 kcal mol^{-1} (ref 14).

(2) (a) Bhogala, B. R.; Basavoju, S.; Nangia, A. Three-Component Carboxylic Acid-Bipyridine Lattice Inclusion Host. Supramolecular Synthesis of Ternary Cocrystals. *Cryst. Growth Des.* **2005**, *5*, 1683−1686. (b) Shattock, T. R.; Vishweshwar, P.; Zang, Z.; Zaworotko, M. J. 18-Fold Interpenetration and Concomitant Polymorphism in the 2:3 Co-crystal of Trimesic Acid and 1,2-Bis(4-pyridyl)ethane. *Cryst. Growth Des.* **2005**, *5*, 2046−2049. (c) Aakeröy, C. B.; Desper, J.; Urbina, J. F. Supramolecular Reagents: Versatile Tools for Non-Covalent Synthesis. *Chem. Commun.* **2005**, 2820−2822. (d) Aakeröy, C. B.; Desper, J.; Urbina, J. F. Balancing Supramolecular Reagents for Reliable Formation of Co-crystals. *Chem. Commun.* **2006**, 1445−1447. (e) Aakeröy, C. B.; Beatty, A. M.; Helfrich, B. A. "Total synthesis" Supramolecular Style: Design and Hydrogen-Bond-Directed Assembly of Ternary Supermolecules. *Angew. Chem., Int. Ed.* **2001**, *40*, 3240−3242. (f) Bhogala, B. R.; Nangia, A. Cocrystals of 1,3,5-Cyclohexanetricarboxylic Acid with 4,4′ -Bipyridine Homologues: Acid···pyridine Hydrogen Bonding in Neutral and Ionic Complexes. *Cryst. Growth Des.* **2003**, *3*, 547−554. (g) Vishweshwar, P.; Nangia, A.; Lynch, V. M. Molecular Complexes of Homologous Alkanedicarboxylic Acids with Isonicotinamide: X-ray Crystal Structures, Hydrogen Bond Synthons, and Melting Point Alternation. *Cryst. Growth Des.* **2003**, *3*, 783−790. (h) Cheung, E. Y.; Kitchin, S. J.; Harris, K. D. M.; Imai, Y.; Tajima, N.; Kuroda, R. Direct Structure Determination of a Multicomponent Molecular Crystal Prepared by a Solid-State Grinding Procedure. *J. Am. Chem. Soc.* **2003**, *125*, 14658−14659. (i) Gao, X.; Friščić, T. T.; MacGillivray, L. R. Supramolecular Construction of Molecular Ladders in the Solid State. *Angew. Chem., Int. Ed.* **2004**, *43*, 232−236. (j) Reddy, L. S.; Nangia, A.; Lynch, V. M. Phenyl−Perfluorophenyl Synthon Mediated Cocrystallization of Carboxylic Acids and Amides. *Cryst. Growth Des.* **2004**, *4*, 89−94.

(3) (a) Desiraju, G. R. Crystal and Co-crystal. *CrystEngComm* **2003**, *5*, 466−467. (b) Dunitz, J. D. Crystal and Co-crystal: A Second Opinion. *CrystEngComm* **2003**, *5*, 506.

(4) (a) Almarsson, Ö.; Zaworotko, M. J. Crystal Engineering of the Composition of Pharmaceutical Phases. Do Pharmaceutical Co-crystals Represent a New Path to Improved Medicines? *Chem. Commun.* **2004**, 1889−1896. (b) Aakeröy, C. B.; Salmon, D. J. Building Co-crystals with Molecular Sense and Supramolecular Sensibility. *CrystEngComm* **2005**, *7*, 439−448. (c) Bhogala, B. R.; Basavoju, S.; Nangia, A. Tape and Layer Structures in Cocrystals of Some Di- and Tricarboxylic Acids with 4,4′-Bipyridines and Isonicotinamide. From Binary to Ternary Co-crystals. *CrystEngComm* **2005**, *7*, 551−562.

(5) (a) Metrangolo, P.; Neukirch, H.; Pilati, T.; Resnati, G. Halogen Bonding Based Recognition Processes: A World Parallel to Hydrogen Bonding. *Acc. Chem. Res.* **2005**, *38*, 386−395. (b) Nguyen, H. L.; Horton, P. N.; Hursthouse, M. B.; Legon, A. C.; Bruce, D. W. Halogen Bonding: A New Interaction for Liquid Crystal Formation. *J. Am. Chem. Soc.* **2004**, *126*, 16−17.

(6) (a) Coates, G. W.; Dunn, A. R.; Henling, L. M.; Dougherty, D. A.; Grubbs, R. H. Phenyl-Perfluorophenyl Stacking Interactions: A New Strategy for Supermolecule Construction. *Angew. Chem., Int. Ed. Engl.* **1997**, *36*, 248−251. (b) Collings, J. C.; Roscoe, K. P.; Thomas, R. L.; Batsanov, A. S.; Stimson, L. M.; Howard, J. A. K.; Marder, T. B. Arene-Perfluoroarene Interactions in Crystal Engineering. Part 3. Single-Crystal Structures of 1:1 Complexes of Octafluoronaphthalene with Fused-ring Polyaromatic Hydrocarbons. *New J. Chem.* **2001**, *25*, 1410−1417. (c) Vangala, V. R.; Nangia, A.; Lynch, V. M. Interplay of Phenyl-Perfluorophenyl Stacking, C−H···F, C−F···π and F···F interactions in Some Crystalline Aromatic Azines. *Chem. Commun.* **2002**, 1304−1305.

Scheme 3. Synthesis of Cocrystals **1**−**10** from Carboxamide and Pyridine *N*-Oxide Molecules[a]

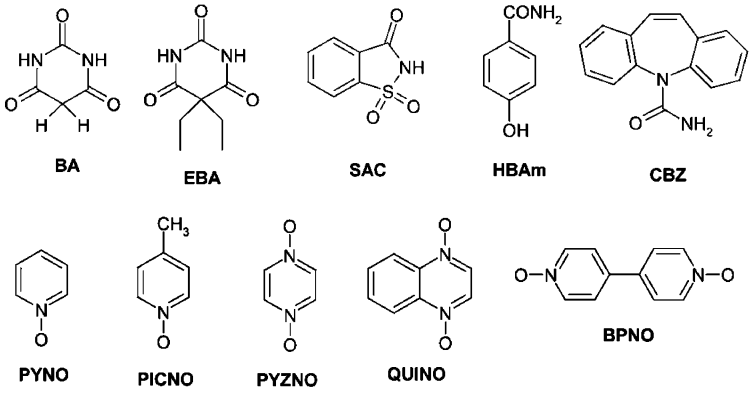

BA•QUINO (1:1) (1)	**BA•PICNO (1:2) (2)**	**BA•PYZNO (1:0.5) (3)**	**SAC•BPNO (1:0.5) (4)**
EBA•PYNO (1:1) (5)	**EBA•PICNO (1:2) (6)**	**HBAm•BPNO (1:0.5) (7)**	**HBAm•PYRNO•H_2O (1:0.5:1) (8)**
CBZ•QUINO (1:1) (9)	**CBZ•PYZNO (1:0.5) (10)**		

[a] Abbreviations for molecular components are used in the paper, and cocrystal stoichiometry is given in parentheses.

in the final cocrystal the constituent molecules have a composite, homogeneous (single) crystalline entity and hence there is no need for the hyphen. From an English language style[11] co- also indicates a role as in co-chair or co-worker whereas cooperation and coordination polymer are usually written without hyphen. A convenient reason for using the hyphen is to split longer words, e.g., multi-component, anti-cooperative, etc.

Carboxylic acids and carboxamides have traditionally been used in structural chemistry because they readily aggregate through the dimer homosynthon. Acid−pyridine heterosynthon is the most popular and frequently occurring hydrogen bond motif in the Cambridge Structural Database, and has an occurrence probability of over 90%[12] compared to <50% frequency for other strong H bond synthons,[13] such as acid−

(7) (a) Bhogala, B. R.; Vishweshwar, P.; Nangia, A. Equivalence of NH_4^+, $NH_2NH_3^+$ and $OHNH_3^+$ in Directing the Noncentrosymmetric Diamond Network of O−H···O$^-$ Hydrogen Bonds in Dihydrogen Cyclohexanetricarboxylate. *Cryst. Growth Des*. **2005**, *5*, 1271−1281. (b) Bhogala, B. R.; Nangia, A. Influence of the Ammonium Cation and 18-crown-6 Guest on the Supramolecular Networks of 1,3,5-Cyclohexanetricarboxylic Acid. *Cryst. Growth Des*. **2006**, *6*, 32−35.

(8) (a) Reddy, L. S.; Bhatt, P.; Banerjee, R.; Nangia, A.; Kruger, G. J. Variable-Temperature Powder X-ray Diffraction of Aromatic Carboxylic Acids and Carboxamide Cocrystals. *Chem. Asian J.* **2007**, *2*, 505−513. (b) See CrystEngWiki for Cocrystal terminology, http://www.rsc.org/Publishing/Community/News/CrystEngWiki.asp.

(9) (a) Walsh, R. D. B.; Bradner, M. W.; Fleischman, S.; Morales, L. A.; Moulton, B.; Rodríguez-Hornedo, N.; Zaworotko, M. J. Crystal Engineering of the Composition of Pharmaceutical Phases. *Chem. Commun.* **2003**, 186−187. (b) Remenar, J. F.; Morissette, S. L.; Peterson, M. L.; Moulton, B.; MacPhee, J. M.; Guzman, H. R.; Almarsson, O. Crystal Engineering of Novel Cocrystals of a Triazole Drug with 1,4-Dicarboxylic Acids. *J. Am. Chem. Soc.* **2003**, *125*, 8456−8457. (c) Vishweshwar, P.; McMahon, J.; Peterson, M. L.; Hickey, M. B.; Shattock, T. R.; Zaworotko, M. J. Crystal Engineering of Pharmaceutical Co-crystals from Polymorphic Active Pharmaceutical Ingredients. *Chem. Commun.* **2005**, 4601−4603. (d) Chen, A. M.; Ellison, M. E.; Peresypkin, A.; Wenslow, R. M.; Variankaval, N.; Savarin, C. G.; Natishan, T. K.; Mathre, D. J.; Dormer, P. G.; Euler, D. H.; Ball, R. G.; Ye, Z.; Wang, Y.; Santos, I. Development of a Pharmaceutical Cocrystal of a Monophosphate Salt with Phosphoric Acid. *Chem. Commun.* **2007**, 419−421. (e) Vishweshwar, P.; McMahon, J. A.; Bis, J. A.; Zaworotko, M. J. Pharmaceutical Co-crystals. *J. Pharma. Sci*. **2006**, *95*, 499−516. (f) Nehm, S. J.; Rodríguez-Spong, B.; Rodríguez-Hornedo, N. Phase Solubility Diagrams of Cocrystals are Explained by Solubility Product and Solution Complexation. *Cryst. Growth Des.* **2006**, *6*, 592−600.

(10) (a) Vishweshwar, P.; McMahon, J. A.; Oliveira, M.; Peterson, M. L.; Zaworotko, M. J. The Predictably Elusive Form II of Aspirin. *J. Am. Chem. Soc.* **2005**, *127*, 16802−16803 (see also ref 10e). (b) Day, G. M.; Trask, A. V.; Motherwell, W. D. S.; Jones, W. Investigating the Latent Polymorphism of Maleic Acid. *Chem. Commun.* **2006**, 54−56. (c) Rafilovich, M.; Bernstein, J. Serendipity and Four Polymoprhic Structures of Benzidine, $C_{12}H_{12}N_2$. *J. Am. Chem. Soc.* **2006**, *128*, 12185. (d) Ahn, S.; Guo, F.; Kariuki, B. M.; Harris, K. D. M. Abundant Polymorphism in a System with Multiple Hydrogen-Bonding Opportunities: Oxalyl Dihydrazide. *J. Am. Chem. Soc.* **2006**, *128*, 8441. (e) Bond, A. D.; Boese, R.; Desiraju, G. R. On the Polymorphism of Aspirin. *Angew. Chem., Int. Ed.* **2007**, *46*, 615.

(11) (a) See http://en.wikipedia.org/wiki/Hyphen and http://en.wikipedia.org/wiki/AP_style. (b) Certain words have very different meaning with and without the hyphen, e.g., recreation (fun) and re-creation (build again), or predate (as in predator) and pre-date (earlier date). This is certainly not the case in co-crystal and cocrystal; both words convey the same meaning.

(12) (a) Steiner, T. Competition of Hydrogen-Bond Acceptors for the Strong Carboxyl Donor. *Acta Crystallogr.* **2001**, B*57*, 103−106. (b) McMahon, J. A.; Bis, J. A.; Vishweshwar, P.; Shattock, T. R.; McLaughlin, O. L.; Zaworotko, M. J. Crystal Engineering of the Composition of Pharmaceutical Phases. Primary Amide Supramolecular Heterosynthons and their Role in the Design of Pharmaceutical Co-crystals. *Z. Kristallogr.* **2005**, *220*, 340−350.

Table 1. Co-Crystallization Conditions for Products **1**−**10**

cocrystal stoichiometry	component 1	component 2	method of crystallization
BA·QUINO (**1**) (1:1)	barbituric acid, 40 mg (0.312 mmol)	quinoxaline *N*,*N*′-dioxide, 50.6 mg (0.312 mmol)	Grind in mortar−pestle for 5 min, add 5 drops of MeCN, dissolved in 10 mL of MeCN. Crystals after 2−3 days at rt.
BA·PICNO (**2**) (1:2)	barbituric acid, 50 mg (0.390 mmol)	4-methylpyridine *N*-oxide, 85 mg (0.780 mmol)	Dissolve in 6−8 mL of THF, allowed to evaporate over 3−4 days.
BA·PYZNO (**3**) (1:0.5)	barbituric acid, 50 mg (0.390 mmol)	pyrazine *N*,*N*′-dioxide, 44 mg (0.390 mmol)	Dissolved in 3 mL of water, allowed to evaporate over 3−4 days.
SAC·BPNO (**4**) (1:0.5)	saccharin, 50 mg (0.272 mmol)	bipyridine *N*,*N*′-dioxide, 26 mg (0.136 mmol)	Ground in mortar−pestle for 5 min, added 5 drops of MeCN, dissolved in 10−15 mL of MeCN. Slow evaporation over 2−3 days.
EBA·PYNO (**5**) (1:1)	barbital, 50 mg (0.271 mmol)	pyridine *N*-oxide, 51 mg (0.543 mmol)	Dissolved in 5−8 mL of EtOAc, allowed to evaporate over 3−4 days.
EBA·PICNO (**6**) (1:2)	barbital, 50 mg (0.271 mmol)	picoline *N*-oxide, 59 mg (0.543 mmol)	Dissolved in 5−8 mL of EtOAc, allowed to evaporate over 3−4 days.
HBAm·BPNO (**7**) (1:0.5)	4-hydroxybenzamide, 37 mg (0.265 mmol)	bipyridine *N*,*N*′-dioxide, 50 mg (0.265 mmol)	Dissolved in 5 mL of acetone/MeOH/water (5 + 5 + 2 mL), allowed to evaporate slowly in 25 mL beaker.
HBAm·PYZNO·H_2O (**8**) (1:0.5:1)	4-hydroxybenzamide, 54 mg (0.392 mmol)	pyrazine *N*,*N*′-dioxide, 40 mg (0.392 mmol)	Dissolved in 5 mL of water, allowed to evaporate slowly in 25 mL beaker over 3−4 days.
CBZ·QUINO (**9**) (1:1)	carbamazepine, 50 mg (0.211 mmol)	quinoxaline *N*,*N*′-dioxide, 22.4 mg (0.106 mmol)	Mortar−pestle + MeCN slurry grinding, solid product dissolved in 8 mL of MeCN, evaporated over 3−4 days.
CBZ·PYZNO (**10**) (1:0.5)	carbamazepine, 80 mg (0.339 mmol)	pyrazine *N*,*N*′-dioxide, 19 mg (0.169 mmol)	Mortar−pestle MeCN slurry grinding, solid dissolved in 5 mL of DMF, evaporated over 3−4 days.

acid, amide−amide, and acid−amide (Scheme 1). Strong and directional hydrogen bonds have been used in rational strategies to design binary/ternary cocrystals for crystal engineering, materials science, host−guest inclusion compounds, and pharmaceutical solids.[2,4] We recently reported a novel heterosynthon,[14] the amide−*N*-oxide motif, by taking advantage of a strong N−H···O^- hydrogen bond. Pyridine *N*-oxide (N^+-O^-) is a stronger acceptor than pyridyl N because of its anionic character. For example, pK_{HB} values[15] of pyridine N, amide O, and *N*-oxide O^- are 1.86, 1.96, and 2.70 (increasing basicity) and, moreover, electrostatic surface potential (ESP) charges at the electronegative atoms (e.g., isonicotinamide, N −43.7, O −47.4 kcal mol^{-1}; isonicotinamide *N*-oxide, O^- −53.3, O −43.1 kcal mol^{-1}) parallel the same trend. In terms of energy, the amide−*N*-oxide two-point heterosynthon of N−H···O^- and C−H···O hydrogen bonds is ca. 3 kcal mol^{-1} more stable than the constituent amide dimer and pyridine *N*-oxide homosynthons of N−H···O and C−H···O^- H bonds (Scheme 2).[16]

We discuss in this paper X-ray crystal structures of carboxamide and pyridine *N*-oxide cocrystals to assess the robustness and breadth of amide−*N*-oxide and amide dimer synthons in pharmaceutical solids.

Table 2. IR Stretching Frequency (KBr, cm^{-1}) of N−H Group in Pyridine *N*-Oxides Compared to Starting Pyridyl−Amides

pyridine amide	pyridine *N*-oxide amide
SAC 3398	SAC·PICNO 3258
BA 3182, 3096	BA·QUINO (**1**) 3097, 3005
BA 3182, 3096	BA·PICNO (**2**) 3107, 3028
BA 3182, 3096	BA·PYZNO (**3**) 3082
SAC 3398	SAC·BPNO (**4**) 3258
EBA 3242, 3109	EBA·PYNO (**5**) 3000
EBA 3242, 3109	EBA·PICNO (**6**) 3076, 2980
CBZ 3466, 3341, 3283, 3163	CBZ·QUINO (**9**) 3368, 3283, 3194, 3080
CBZ 3466, 3341, 3283, 3163	CBZ·PYZNO (**10**) 3350, 3188

Experimental Section

Cocrystal Preparation. Starting materials were purchased from commercial suppliers. Pyridine *N*-oxides were prepared by *m*-CPBA oxidation of the corresponding pyridines.

Cocrystals **1**−**8** (Scheme 3) were obtained by dissolving stoichiometric mixtures of the components in a suitable solvent by gentle warming and allowing single crystals of the binary phase to appear after slow evaporation of solvent at ambient temperature. Cocrystals **9** and **10** however could

(13) Allen, F. H.; Motherwell, W. D. S.; Raithby, P. R.; Shields, G. P.; Taylor, R. Systematic Analysis of the Probabilities of Formation of Bimolecular Hydrogen-Bonded Ring Motifs in Organic Crystal Structures. *New J. Chem.* 1999, 25−34.

(14) Reddy, L. S.; Babu, N. J.; Nangia, A. Carboxamide−Pyridine-*N*-oxide Heterosynthon for Crystal Engineering and Pharmaceutical Cocrystals. *Chem. Commun.* **2006**, 1369−1371.

(15) Laurence, C.; Berthelot, H. Observations on the Strength of Hydrogen Bonding. *Perspect. Drug Discovery Des.* **2000**, *18*, 39−60.

(16) Atomic charges and hydrogen bond energies were calculated in Spartan 04 at RHF/6−31G** level, http://www.wavefun.com. See ref 14 for details.

Table 3. X-ray Crystal Structure Data on Cocrystals **1**−**10**

	BA·QUINO (**1**)	BA·PICNO (**2**)	BA·PYZNO (**3**)	SAC·BPNO (**4**)	EBA·PYNO (**5**)
empirical formula	$(C_4H_4N_2O_3)\cdot(C_8H_6N_2O_2)$	$(C_4H_4N_2O_3)\cdot 2(C_6H_7NO)$	$(C_4H_4N_2O_2)\cdot 0.5(C_4H_4N_2O_3)$	$(C_7H_5NO_3S)\cdot 0.5(C_{10}H_8N_2O_2)$	$(C_8H_{12}N_2O_3)\cdot(C_5H_5NO)$
formula weight	290.24	346.34	184.14	554.54	279.30
cryst syst	monoclinic	triclinic	monoclinic	monoclinic	monoclinic
space group	$P2_1/n$	$P\bar{1}$	$P2_1/n$	$P2_1/n$	$P2_1/c$
T/K	293(2)	293(2)	293(2)	100(2)	293(2)
a/Å	10.3850(9)	8.4083(7)	5.258(3)	6.5207(4)	7.2276(5)
b/Å	7.2222(6)	9.8893(9)	6.478(3)	14.0377(9)	19.5811(12)
c/Å	16.3763(14)	10.6761(9)	22.118(11)	13.1232(9)	9.9928(6)
α/deg	90	73.2010(10)	90	90	90
β/deg	93.6860(10)	79.022(2)	95.795(8)	104.2800(10)	98.1360(10)
γ/deg	90	74.182(2)	90	90	90
Z	4	2	4	4	4
V/Å^3	1225.72(18)	811.64(12)	749.5(7)	1164.12(13)	1399.99(15)
D_{calc}/g cm^{-3}	1.573	1.417	1.632	1.582	1.325
μ/mm^{-1}	0.126	0.107	0.140	0.290	0.100
reflns collected	12226	6726	7435	6302	10123
unique reflns	2410	3187	1511	2288	2750
obsd reflns	1898	2369	1390	2024	2413
$R_1[I > 2\sigma(I)]$	0.0381	0.0516	0.0434	0.0362	0.0398
wR_2 [all]	0.1018	0.1316	0.1079	0.0954	0.1116
GOF	1.03	1.04	1.06	1.08	1.04
diffractometer	SMART-APEX CCD	SMART-APEX CCD	SMART-APEX CCD	SMART-APEX CCD	SMART-APEX CCD

	EBA·PICNO (**6**)	HBAm·BPNO (**7**)	HBAm·PYZNO hydrate (**8**)	CBZ·QUINO (**9**)	CBZ·PYZNO (**10**)
empirical formula	$(C_8H_{12}N_2O_3)\cdot 2(C_6H_7NO)$	$(C_7H_7NO_2)\cdot 0.5(C_{10}H_8N_2O_2)$	$(C_7H_7NO_2)\cdot 0.5(C_4H_4N_2O_2)\cdot H_2O$	$(C_{15}H_{12}N_2O)\cdot(C_8H_6N_2O_2)$	$(C_{15}H_{12}N_2O)\cdot 0.5(C_4H_4N_2O_2)$
formula weight	402.45	462.46	211.20	398.41	292.31
cryst syst	monoclinic	triclinic	triclinic	triclinic	monoclinic
space group	$P2_1/c$	$P\bar{1}$	$P\bar{1}$	$P\bar{1}$	$P2_1/c$
T/K	100(2)	293(2)	293(2)	293(2)	293(2)
a/Å	8.2106(5)	5.692(4)	6.409(4)	7.284(2)	10.237(4)
b/Å	23.9166(15)	9.482(6)	7.372(4)	10.688(4)	27.247(12)
c/Å	20.6318(13)	10.751(7)	11.064(6)	14.132(5)	5.135(2)
α/deg	90	69.893(10)	96.127(14)	100.250(5)	90
β/deg	96.6700(10)	84.232(10)	97.22(3)	102.463(5)	102.708(7)
γ/deg	90	84.969(10)	105.350(9)	109.079(5)	90
Z	8	2	2	2	4
V/Å^3	4024.0(4)	541.2(6)	497.7(5)	977.8(6)	1397.2(10)
D_{calc}/g cm^{-3}	1.329	1.419	1.418	1.353	1.390
μ/mm^{-1}	0.097	0.104	0.112	0.092	0.094
reflns collected	25727	5499	3642	9904	14153
unique reflns	7922	2133	1948	3808	2789
obsd reflns	4351	1518	1210	2757	2339
$R_1[I > 2\sigma(I)]$	0.0537	0.0455	0.0473	0.0548	0.1380
wR_2 [all]	0.1696	0.1323	0.1309	0.1295	0.2868
GOF	1.01	1.03	0.97	1.06	1.29
diffractometer	SMART-APEX CCD	SMART-APEX CCD	SMART-APEX CCD	SMART-APEX CCD	SMART-APEX CCD

not be obtained by the solution crystallization method. Solid-state grinding in mortar−pestle or mechanical ball mill did not give product cocrystals. Addition of CH_3CN (1−3 mL) to the starting materials and grinding the slurry for 5−10 min gave complete conversion to the desired cocrystal after evaporation of the solvent. Attempts with increasing the temperature of the solid-state reaction or melt cocrystallization[8a] did not yield successful results. Crystallization scale and conditions are summarized in Table 1. Adduct formation was monitored by changes in amide NH infrared spectrum bands from starting materials to product cocrystal[14] (Table 2).

X-ray Crystal Structure. X-ray data on cocrystals **1**−**10** were collected on Bruker-Nonius SMART-APEX CCD diffractometer (Mo Kα radiation, $\lambda = 0.710\ 73$ Å). RLATT3 and CELL_NOW programs[17] were used to generate a new reindexed cell for cocrystal **6**, which was used during initialization and merging of raw data. Crystal structures were

Table 4. Hydrogen Bond Distance and Angle Parameters (Neutron-Normalized N−H, O−H, and C−H Distances)

cocrystal	H bond	H···A/Å	D···A/Å	∠D−H···A/deg	cocrystal	H bond	H···A/Å	D···A/Å	∠D−H···A/deg
1	N3−H3···O3	1.93	2.935(1)	176	**6**	N1−H1···O8	1.75	2.742(3)	167
	N4−H4···O2	1.75	2.757(1)	174		N2−H2···O7	1.74	2.735(3)	170
	C1−H1···O3	2.34	3.341(1)	154		N3−H3···O6	1.74	2.733(3)	166
	*C*2−H2···O5	2.11	3.189(2)	173		N4−H4···O5	1.74	2.743(3)	172
	C5−H5···O1	2.28	3.091(2)	130		C17−H17···O7	2.41	3.457(3)	162
	C12−H12A···O1	2.49	3.446(2)	147		C21−H21···O7	2.49	3.548(3)	165
2	N1−H1···O4	1.75	2.746(2)	171		C22−H22B···O8	2.57	3.535(3)	148
	C10−H10···O3	2.13	3.170(2)	160		C23−H23···O8	2.45	3.499(3)	163
	N2−H2···O5	1.80	2.797(2)	171		C27−H27···O8	2.46	3.500(3)	161
	C16−H16···O2	2.29	3.342(3)	164		C28−H28B···O7	2.49	3.528(3)	159
	C4−H4A···O4	2.50	3.514(2)	155		C29−H29···O5	2.49	3.532(3)	162
	C4−H4B···O5	2.40	3.323(2)	143		C33−H33···O5	2.45	3.485(3)	160
	C5−H5···O5	2.14	3.222(2)	174		C34−H34B···O5	2.60	3.547(3)	146
	C6−H6···O2	2.47	3.467(2)	152		C35−H35···O6	2.45	3.513(3)	165
	C8−H8B···O3	2.35	3.287(2)	144		C40−H40···O6	2.43	3.474(3)	162
	C11−H11···O4	2.24	3.312(2)	170	**7**	N1−H1A···O1	1.88	2.892(3)	179
	C12−H12···O2	2.42	3.342(2)	142		N1−H1B···O3	2.07	3.024(3)	158
3	N1−H1···O1	1.80	2.798(2)	172		O2−H2···O3	1.65	2.627(3)	173
	N2−H2···O4	1.78	2.785(2)	172		C8−H8···O2	2.34	3.280(3)	144
	C4−H4A···O2	2.67	3.471(3)	130	**8**	N1−H1A···O1	1.91	2.911(3)	171
	C4−H4A···O1	2.60	3.391(3)	130		N1−H1B···O3	2.01	2.988(3)	162
	C6−H6···O2	2.45	3.437(3)	151		O2−H2···O4	1.69	2.666(3)	174
4	N2−H1···O1	1.68	2.663(2)	163		O4−H4A···O3	1.85	2.822(3)	169
	C4−H4···O1	2.06	3.136(2)	170		O4−H4B···O1	1.75	2.721(3)	170
	C6−H6···O4	2.48	3.434(2)	146		C3−H3···O3	2.54	3.408(3)	136
	C7−H7···O2	2.40	3.361(2)	147		C8−H8···O4	2.52	3.433(4)	142
	C11−H11···O2	2.41	3.109(2)	121		C9−H9···O2	2.15	3.118(3)	148
	C12−H12···O2	2.53	3.163(2)	116	**9**	N1−H1A···O1	1.90	2.910(3)	174
5	N2−H2···O1	1.82	2.821(1)	173		N1−H1B···O3	2.02	2.899(3)	145
	C1−H1···O2	2.39	3.356(1)	148		C12−H12···O4	2.61	3.624(3)	155
	N3−H3···O1	1.87	2.867(1)	172		C14−H14···O1	2.36	3.267(3)	141
	*C*2−H2A···O4	2.44	3.361(2)	142		C16−H16···O3	2.45	3.235(3)	129
	C3−H3A···O3	2.40	3.363(1)	147		C17−H17···O1	2.13	3.145(3)	154
	C5−H5···O3	2.24	3.313(1)	172		C19−H19···O4	2.46	3.309(3)	135
	C11−H11C···O2	2.39	3.421(1)	158	**10**	N1−H1A···O1	1.97	2.940(7)	160
						N1−H1B···O3	2.10	3.034(7)	152
						C14−H14···O1	2.55	3.520(7)	149
						C16−H16···O1	2.37	3.081(7)	121
						C17−H17···O1	2.50	3.134(8)	116

solved by direct methods and refined on F^2 with SHELXS-97 and SHELXL-97 programs[18] to give satisfactory *R* factor (Table 3). X-Seed[19] was used to prepare figures and packing diagrams. Hydroxy and amide hydrogen atoms were located in difference electron density Fourier maps and refined isotropically. Other hydrogen atoms were fixed at geometrically reasonable positions. Hydrogen bond metrics are listed in Table 4.

Hydration Stability. The relative humidity was ca. 50% (in the range 45−55%) under ambient conditions of Hyderabad climate during the experiment period in December 2006 (temperature range 25−35 °C). We performed a qualitative experiment to assess the gross difference in hydration nature of 4-picoline *N*-oxide compared to its cocrystal with barbital wherein the *N*-oxide moiety is engaged in strong bonding with an amide partner. The solid was placed in a petri dish exposed to ambient humidity conditions for the specified period, and IR spectra were recorded to monitor water absorption peaks. The solid was placed in 100 mL beaker that was kept in a closed jar containing distilled water to expose the sample to 100% relative humidity conditions (saturated water vapor).

Crystal Structure Prediction. Lattice energy minimization of experimental structures was carried out using version 4.8 of Cerius[2] molecular modeling environment[20] running

(17) (a) *RLATT*, Reciprocal Lattice Viewer, Version 3.0, Bruker-AXS, **2000**. (b) Sheldrick, G. M. *CELL_NOW*; University of Göttingen: Göttingen, Germany, 2004.

(18) Sheldrick, G. M. *SHELXS-97 and SHELXL-97*, Programs for the Solution and Refinement of Crystal Structures; University of Göttingen: Göttingen, Germany, 1997.

(19) Barbour, L. J. *X-Seed*, Graphical Interface to *SHELX-97* and *POV-Ray*; University of Missouri-Columbia: Columbia, MO, 1999.

(20) Polymorph Predictor and Cerius[2] suite of programs are software products of Accelrys Inc., http://www.accelrys.com.

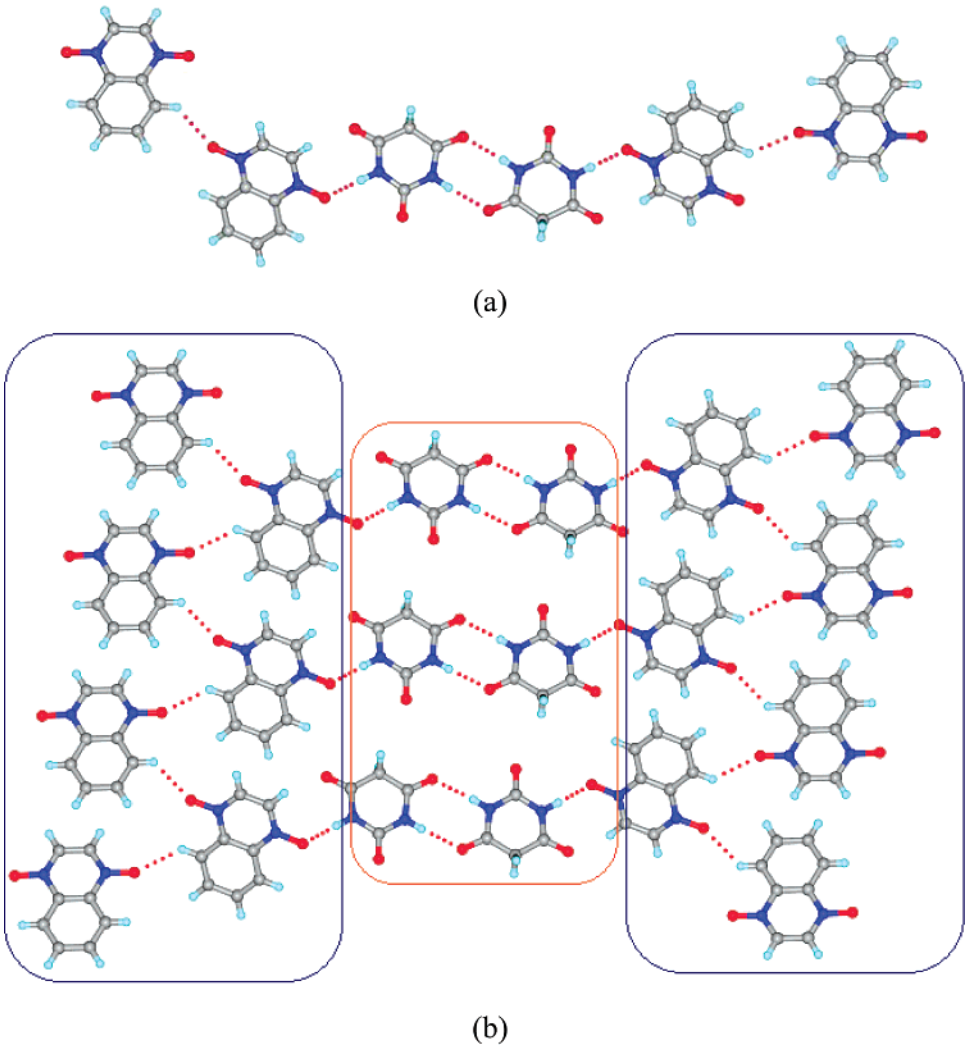

Figure 1. (a) Amide dimer homosynthon between barbituric acid molecules and N−H···O⁻ H bond with quinoxaline *N*,*N*′-dioxide in cocrystal (**1**). (b) Strong N−H···O⁻ H bonds connect C−H···O helices to amide dimers. The two components in the crystal structure are highlighted in red and blue boxes.

on Silicon Graphics workstations. COMPASS force field was applied. The energy minimized molecular structure was used to run rigid conformer polymorph prediction. COSET program[21] was used to analyze predicted frames and to compare the experimental and predicted structures based on rmsd values.

Cambridge Structural Database. CSD version 5.27 (ConQuest 1.9, November 2006 update)[22] was searched for amide and *N*-oxide fragments in organic crystal structures. Out of 186 hits, structures with N−O−H, N−O−C, and piperidine-1-oxy moiety were excluded to give 41 organic hits. These 41 structures were divided into two categories: no strong OH, NH, H_2O groups (27 hits), and strong competing groups are present (14 hits). The amide−*N*-oxide heterosynthon is present in 11/14 structures (7 intra- and 4 intermolecular). Among the 27 refcodes, intramolecular N−H···O⁻ is present in 8 structures, intermolecular N−H···O⁻ bond in another 13 structures, and amide dimer in 5 crystal structures. CSD refcodes are categorized in Table S1 (Supporting Information).

Results and Discussion

The most common method of obtaining cocrystals is to dissolve the components in a suitable solvent system for single crystals of the binary phase to appear after slow evaporation of solvent(s). Gentle warming is necessary to dissolve the solids, and an antisolvent is added to accelerate crystallization. This empirical, trial-and-error method, referred to as solution crystallization, is repeated with several solvents until there is evidence of a new crystalline entity based on DSC, IR, single crystal, and/or powder X-ray diffraction. Precipitation of the individual components instead

(21) COSET is developed and distributed by Cambridge Crystallographic Data Center, http://www.ccdc.cam.ac.uk, chisholm@ccdc.cam.ac.uk.

(22) Cambridge Structural Database, CSD version 5.27, ConQuest 1.9, November 2006 update, http://www.ccdc.cam.ac.uk. Crystal structures were visualized in Mercury 1.5. CSD refcodes of crystal structure statistics discussed in the text are mentioned in the Supporting Information.

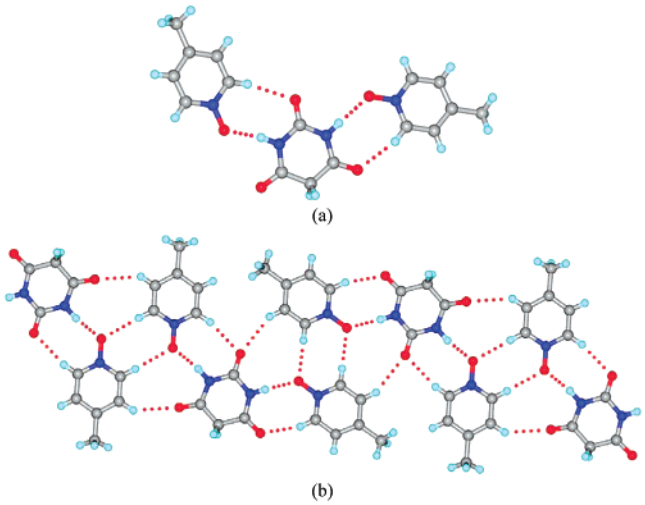

Figure 2. (a) Amide−*N*-oxide heterosynthon connects symmetry-independent barbituric acid and 4-methylpyridine *N*-oxide molecules in cocrystal (**2**). (b) Assembly of a 2D sheet-like structure through C−H···O interactions.

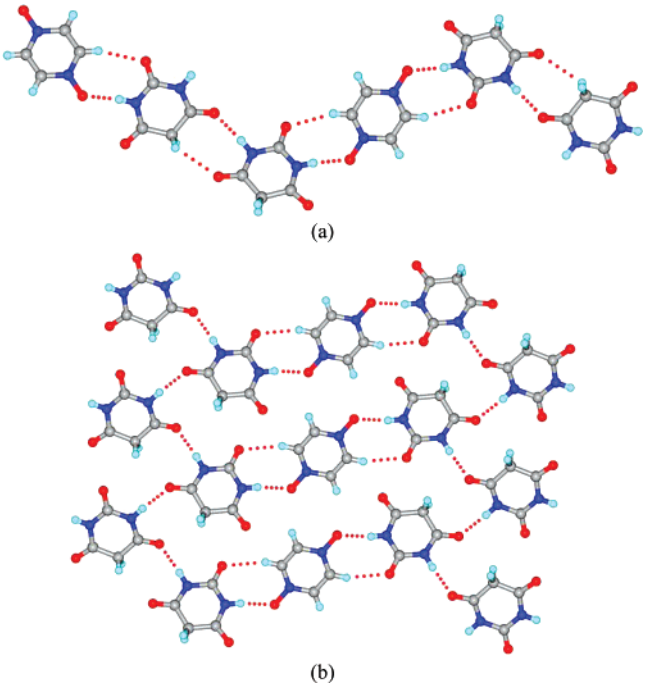

Figure 3. (a) Amide−*N*-oxide heterosynthon generates zigzag tapes of barbituric acid and pyrazine *N,N′*-dioxide molecules in cocrystal **3**. (b) Pyrazine *N,N′*-dioxide molecules (center column) connect helices of barbituric acid on either side. This situation is complementary to that in cocrystal **1** wherein barbituric acid dimers connect helices of quinoxaline *N,N′*-dioxide molecules (Figure 1).

of the desired cocrystal and formation of undesired solvates/hydrates are common difficulties in the solution-based approach. Solid-state grinding[23] overcomes the problem of solvent inclusion, but the product is microcrystalline for routine single-crystal X-ray structure determination. Adding a few drops of solvent during grinding/kneading, referred to as solvent-drop or liquid-assisted grinding, accelerates

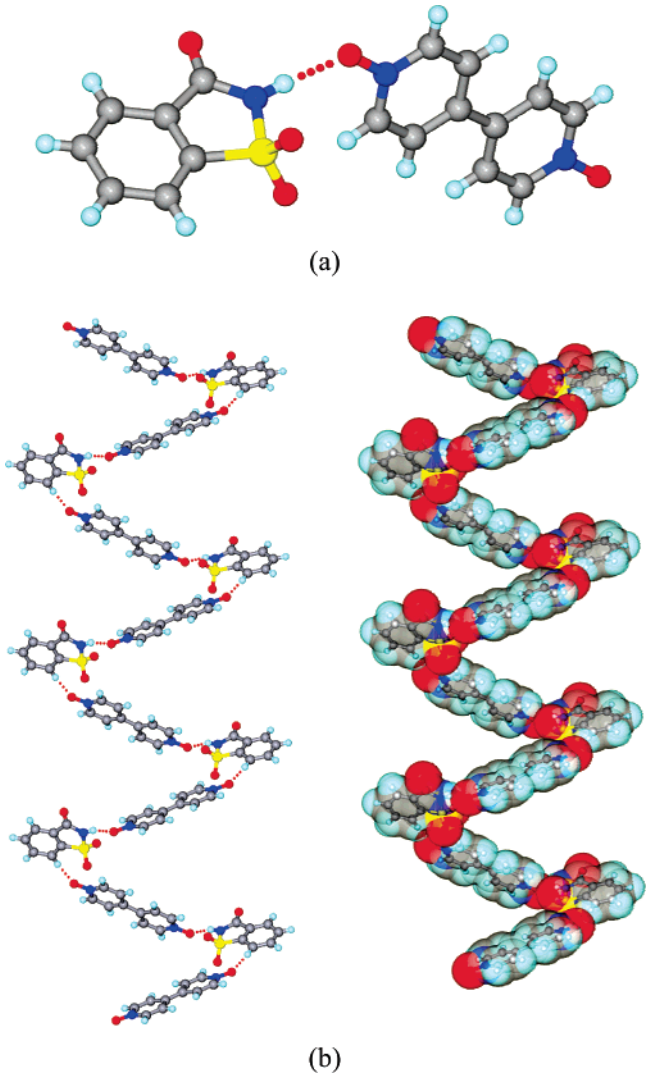

Figure 4. (a) Amide−*N*-oxide heterosynthon between saccharin and 4,4′-bipyridine *N,N′*-dioxide molecules in cocrystal **4**. (b) A helix of molecules via N−H···O$^-$ and C−H···O hydrogen bonds (left, molecular arrangement; right, space-filling view).

adduct formation due to lubrication. Cocrystals **1**−**8** were obtained by the traditional solution crystallization method. However, crystallization from different solvents as well as solid-state or solvent-assisted grinding did not produce cocrystals **9** and **10** of carbamazepine. Upon adding 1−3 mL of acetonitrile to about 100 mg of the solid mixture (CBZ + QUINO, CBZ + PYZNO) and grinding the slurry (compounds were not completely soluble) gave the desired

(23) (a) Trask, A. V.; Jones, W. Crystal Engineering of Organic Cocrystals by the Solid-State Grinding Approach. *Top. Curr. Chem.* **2005**, *254*, 41−70. (b) Trask, A. V.; Motherwell, W. D. S.; Jones, W. Solvent-Drop Grinding: Green Polymorph Control of Cocrystallisation. *Chem. Commun.* **2004**, *7*, 890−891. (c) Friščić, T.; Trask, A.; Jones, W.; Motherwell, W. D. S. Screening for Inclusion Compounds and Systematic Construction of Three-Component Solids by Liquid-Assisted Grinding. *Angew. Chem., Int. Ed.* **2006**, *45*, 7546−7550.

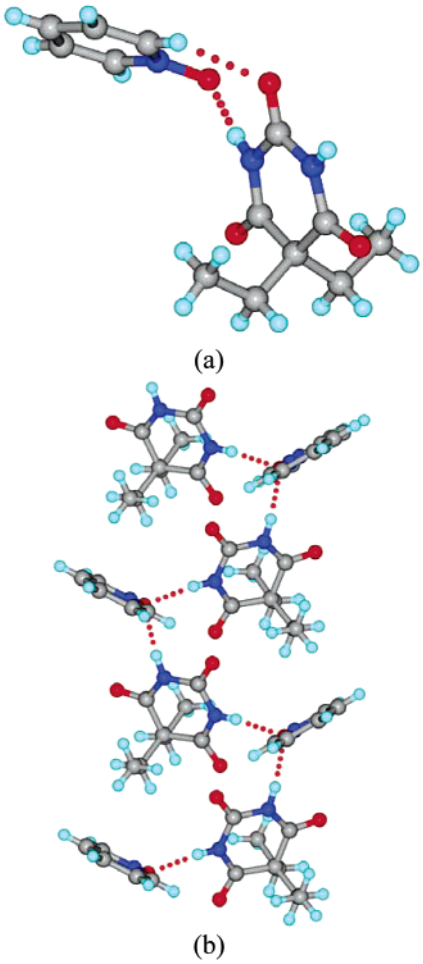

Figure 5. (a) Amide−*N*-oxide heterosynthon between barbital and pyridine *N*-oxide molecules in cocrystal **5**. (b) Helical assembly along the 2-fold screw axis.

cocrystal in each case (see Experimental Section). We refer to this method of cocrystal synthesis as "slurry grinding". ORTEP plots (Figures S1−S10, Supporting Information) of crystal structures **1**−**10** confirmed the molecular stoichiometry of each cocrystal.

Barbituric Acid/Quinoxaline *N,N′*-Dioxide (1). This 1:1 cocrystal crystallized in monoclinic space group $P2_1/n$. Quinoxaline *N,N′*-dioxide molecules form a helix along the *b*-axis via C5−H5···O1 interaction (2.28 Å, 3.091(2) Å, 130°), the distance being relatively short because the interaction is between aromatic C−H donor and electronegative O^- acceptor. Barbituric acid molecules are connected by amide dimer (N3−H3···O3: 1.93 Å, 2.935(1) Å, 176°; Figure 1). There is no amide−*N*-oxide synthon in this crystal structure, but an isolated N4−H4···O2 H bond (1.75 Å, 2.757(1) Å, 174°) connects quinoxaline dioxide C−H···O helices and amide dimers of BA molecules. Miscellaneous C−H···O interactions in the crystal structure are listed in Table 4.

Barbituric Acid/4-Methylpyridine *N*-Oxide (2). This crystal structure in triclinic space group $P\bar{1}$ contains one barbituric acid and two 4-methylpyridine *N*-oxide molecules

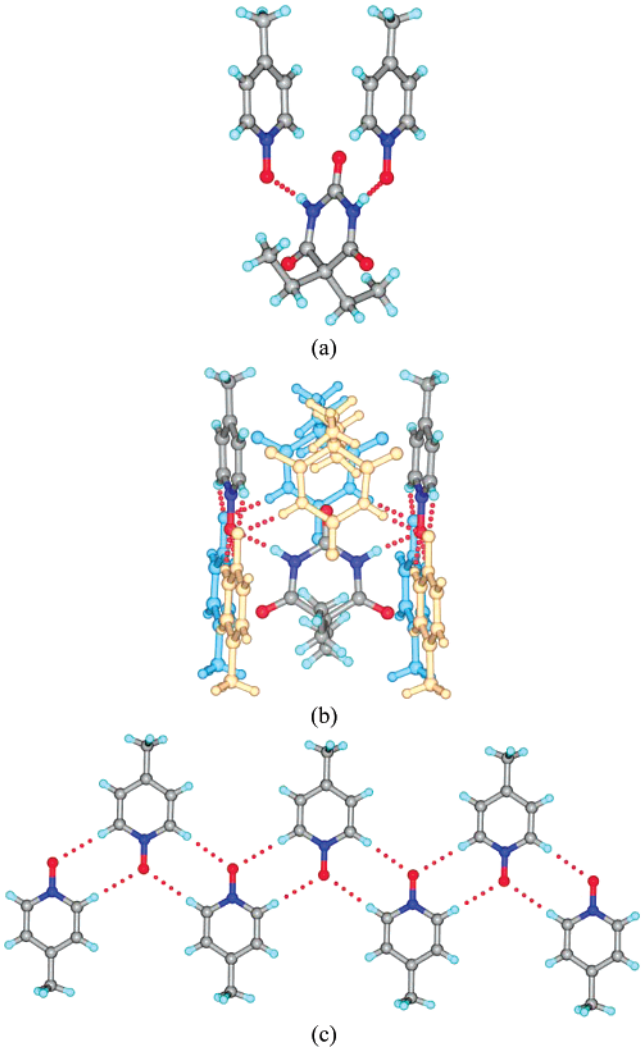

Figure 6. (a) N−H···O^- hydrogen bond between barbital and *N*-oxide molecules. There are two such symmetry-independent clusters in cocrystal **6**. (b) Each three-molecule cluster shown in panel a is flanked by the symmetry-independent cluster of EBA and PICNO, shown in different colors (yellow and blue) for easy viewing of overlapping atoms. (c) Linear tape of picoline *N*-oxide molecules in cocrystal structure. Barbital molecules are not shown for clarity.

consistent with the functional group stoichiometry (Figure 2a). The ternary assembly of PICNO molecules flanked on either side of BA is sustained by amide−*N*-oxide synthons (N1−H1···O4, 1.75 Å, 2.746(2) Å, 171°; N2−H2···O5, 1.80 Å, 2.797(2) Å, 171°). A second symmetry-independent *N*-oxide molecule forms dimers via C5−H5···O5 (2.14 Å, 3.222(2) Å, 174°) and C11−H11···O4 (2.24 Å, 3.312(2) Å, 170°) interactions. These motifs repeat in the crystal structure (Figure 2b) to generate a 2D sheet structure.

Barbituric Acid/Pyrazine *N,N′*-Dioxide (3). The crystal structure (space group $P2_1/n$) contains one barbituric acid and half pyrazine *N,N′*-dioxide molecule in the asymmetric unit. PYZNO molecules reside at the inversion center and participate in amide−*N*-oxide synthon with BA amide group (N2−H2···O4, 1.78 Å, 2.785(2) Å, 172°; C6−H6···O2, 2.45

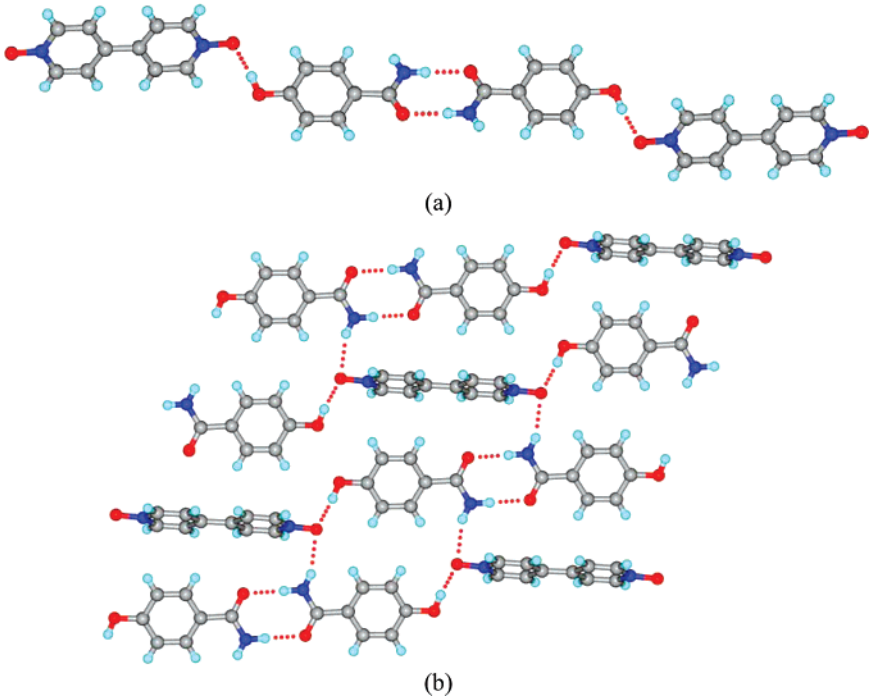

Figure 7. (a) 1D tape of amide dimer homosynthon and N−H···O$^-$ hydrogen bond in cocrystal **7**. (b) Herringbone type packing between phenyl rings in the crystal structure.

Å, 3.437(3) Å, 151°). The molecules extend in 1D zigzag tape through N1−H1···O1 hydrogen bond (1.80 Å, 2.798(2) Å, 172°) and C4−H4A···O2 interaction (2.67 Å, 3.471(3) Å, 130°). BA assemble in a helix of N1−H1···O1 interaction along the *b*-axis, and PYZNOs act as a bridges to connect inversion related helices using C−H···O interactions (Figure 3).

Saccharin/4,4′-Bipyridine *N,N′*-Dioxide (4). It crystallized in the monoclinic space group $P2_1/n$ with one SAC and half BPNO molecule in the asymmetric unit, as expected from functional group stoichiometry of partner molecules. A strong N2−H1···O1 hydrogen bond (1.68 Å, 2.663(2) Å, 163°) connects component molecules in the cocrystal (Figure 4). The *N*-oxide acceptor is involved in bifurcated C4−H4···O1 interaction (2.06 Å, 3.136(2) Å, 170°) with an aromatic C−H donor to generate helices along the *b*-axis. A larger helix is revealed when BPNOs residing at the inversion center and SAC molecules are considered. A 1:1 cocrystal of saccharin and 4-picoline *N*-oxide was prepared recently.[24]

Diethyl Barbituric Acid (Barbital)/Pyridine *N*-Oxide (5). It crystallized in monoclinic space group $P2_1/c$ with one molecule each of EBA and PYNO in the asymmetric unit. Amide−*N*-oxide heterosynthon (N2−H2···O1, 1.82 Å, 2.821(1) Å, 173°; C1−H1···O2, 2.39 Å, 3.356(1) Å, 148°) and H bonding of PYNO with the second amide N−H donor of EBA (N3−H3···O1: 1.87 Å, 2.867(1) Å, 172°) produce a helical assembly along the *b*-axis (Figure 5).

Barbital/4-Methylpyridine *N*-Oxide (6). The cocrystal crystallized in monoclinic space group $P2_1/c$. The 1:2 stoichiometry of EBA and PICNO in **6** (Figure 6a, 2 and 4 symmetry-independent molecules, respectively) is consistent with their functional group ratio. Four PICNO molecules accept N−H···O$^-$ bonds from two EBA molecules (Figure 6b, N1−H1···O8, 1.75 Å, 2.742(3) Å, 167°; N2−H2···O7, 1.74 Å, 2.735(3) Å, 170°; N3−H3···O6, 1.74 Å, 2.733(3) Å, 166°; N4−H4···O5, 1.74 Å, 2.743(3) Å, 172°). Picoline *N*-oxide molecules aggregate as tapes through C−H···O interactions along the *a*-axis (Figure 6c). Sheets of PICNO molecules parallel to the *ab*-plane intercalate barbital molecules through N−H···O$^-$ H bonds. The molecular layer arrangement along the *c*-axis (repeat units of Figure 6b) is PICNO−EBA−PICNO−PICNO−EBA and so on.

4-Hydroxybenzamide/4,4′-Bipyridine *N,N′*-Dioxide (7). The cocrystal structure in triclinic space group $P\bar{1}$ contains one 4-hydroxybenzamide and half bipyridine dioxide molecules in the asymmetric unit. This cocrystal was synthesized to study the influence of a competing hydroxyl group on the amide group during self-assembly. Now the amide assembles via dimer homosynthon (N1−H1A···O1: 1.88 Å, 2.892(3) Å, 179°) whereas *N*-oxide H bonds with the hydroxyl group (O2−H2···O3: 1.65 Å, 2.627(3) Å, 173°). The electronegative *N*-oxide accepts bifurcated H bond from amide *anti* N−H donor (N1−H1B···O3: 2.07 Å, 3.024(3) Å, 158°) as shown in Figure 7.

4-Hydroxybenzamide/Pyrazine *N,N′*-Dioxide Hydrate (8). Continuing from cocrystal (**7**), hydroxybenzamide and pyrazine dioxide were co-crystallized but now the structure contains an additional water molecule. It crystallized in

(24) Saha, B. K.; Banerjee, R.; Nangia, A. Desiraju, G. R. A 1:1 Molecular Complex of 4-Methylpyridine *N*-oxide and Saccharin. *Acta Crystallogr*. **2006**, E*62*, o2283−o2284.

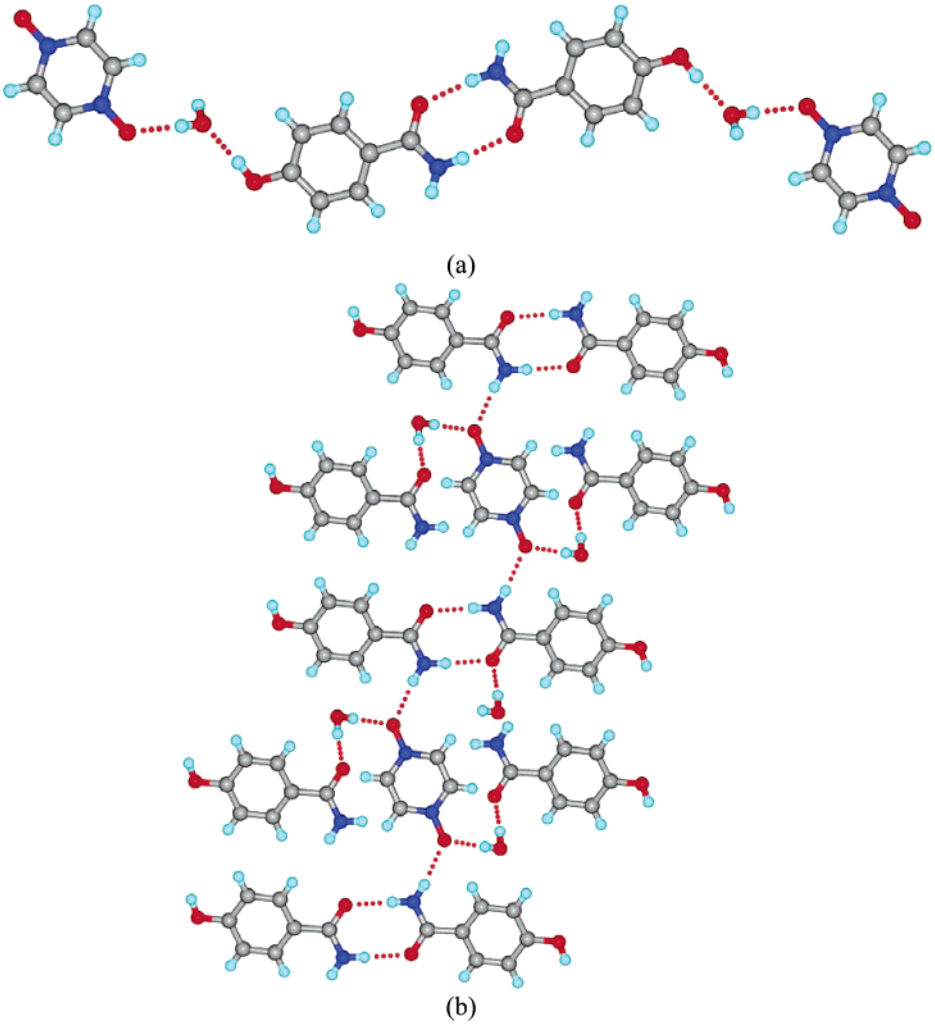

Figure 8. (a) 1D tape of amide dimer homosynthon and water interrupted hydroxyl to *N*-oxide hydrogen bonds in cocrystal **8**. (b) Extended H bonding in the three-component crystal structure.

triclinic space group $P\bar{1}$ with one HBAm, half PYZNO, and one water molecule in the asymmetric unit. The O3 water atom of monohydrate (**8**) interrupts the hydroxyl to *N*-oxide H bond (O4−H4A···O3, 1.85 Å, 2.822(3) Å, 169°, O2−H2···O4, 1.69 Å, 2.666 Å, 174°). Amide dimer homosynthon (N1−H1A···O1: 1.91 Å, 2.911(3) Å, 171°) and *anti* N−H donating to *N*-oxide (N1−H1B···O3: 2.01 Å, 2.988-(3) Å, 162°) complete the strong hydrogen bond network in the ternary cocrystal (Figure 8). We noted inclusion of water in barbituric acid·BPNO cocrystal.[14]

Carbamazepine/Quinoxaline *N,N′*-Dioxide (9). This molecular compound crystallized in triclinic space group $P\bar{1}$ with one molecule each in the asymmetric unit. A centrosymmetric amide dimer is formed between inversion-related CBZ molecules using *syn* N−H donor (N1−H1A···O1: 1.90 Å, 2.910(3) Å, 174°). CBZ *anti* N−H donates to an *N*-oxide of QUINO (N1−H1B···O3: 2.02 Å, 2.899(3) Å, 145°). Adjacent CBZ dimers are connected via *N*-oxide cocrystal-former molecules (Figure 9). There is a C−H···O dimer (C16−H16···O3: 2.45 Å, 3.235(3) Å, 129°) between inversion-related *N*-oxide molecules which fill the voids between amide dimers in the structure. These two N1−H1A···O1 and C16−H16···O3 dimers alternate along the *b*-axis and extend in a 2D motif. The second *N*-oxide moiety is also involved in C−H···O dimer (C19−H19···O4: 2.46 Å, 3.309(3) Å, 135°) to connect layers of CBZ dimers. Cocrystal **9** is similar to CBZ−4,4′-bipyridine 2:1 cocrystal.[12b] A difference between **9** and CBZ·BIPY cocrystal is that two QUINO molecules fill the space between CBZ dimers compared to one long BIPY spacer. Accordingly their stoichiometry is 1:1 and 2:1 respectively.

Zaworotko[25] classified hydrogen-bonding changes in going from single component to cocrystal structure in two categories. The first type is when the cocrystal former acts only as a spacer but the original homosynthon is retained. Both CBZ·quinoxaline *N,N′*-dioxide and CBZ·4,4′-bipyridine belong to category 1. On the other hand, when there is substantial change in H bonding because of cocrystal former functional

(25) Fleischman, S. G.; Kuduva, S. S.; McMahon, J. A.; Moulton, B.; Walsh, R. D. B.; Rodríguez-Hornendo, N.; Zaworotko, M. J. Crystal Engineering of the Composition of Pharmaceutical Phases: Multiple-Component Crystalline Solids Involving Carbamazepine. *Cryst. Growth Des.* **2003**, *3*, 909−919.

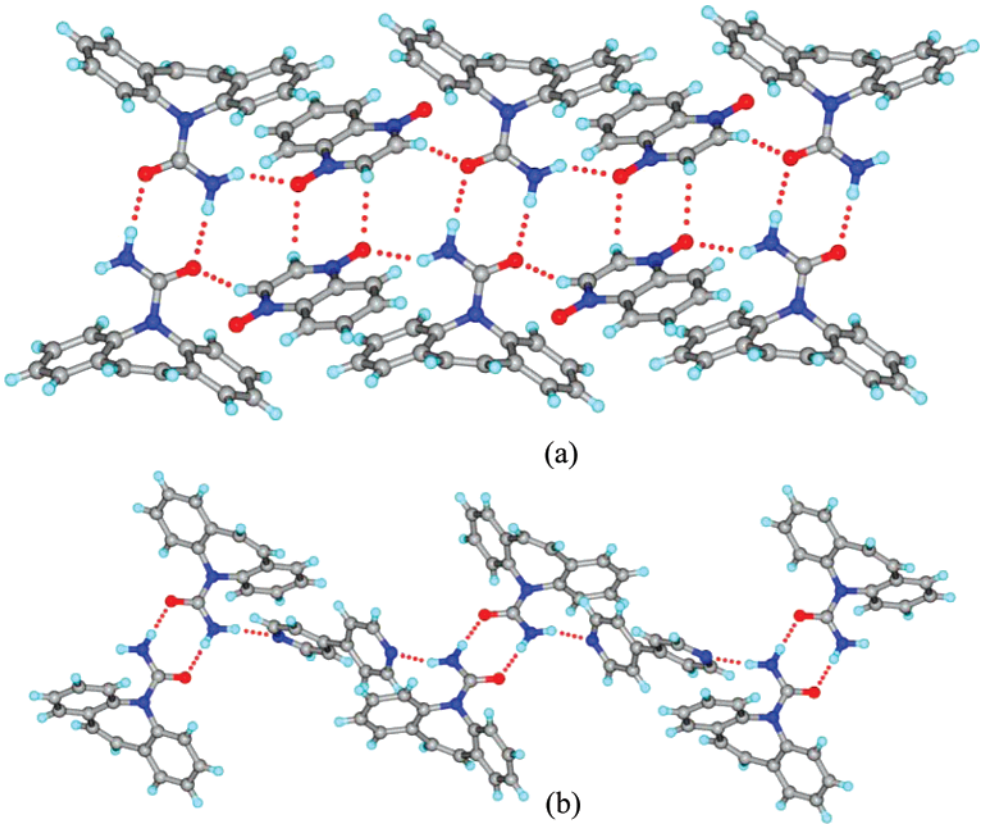

Figure 9. (a) Hydrogen-bonded dimers of CBZ are connected by *anti* N−H···O⁻ H bonds to quinoxaline dioxide and C−H···O dimer of QUINO. Crystal structure **9** is similar to the CBZ·4,4′-bipyridine cocrystal shown in panel b (CSD refcode XAQQUC).

groups, e.g., acid or amide dimer homosynthon changing to acid−pyridine, amide−acid, or amide−*N*-oxide heterosynthon, then the structure belongs to strategy 2. Because of significant structural differences in going from homo- to heterosynthon, second category structures are more likely to result in significant differences in solid-state properties for API cocrystals.

Carbamazepine and Pyrazine *N,N′*-Dioxide (10). It crystallized in monoclinic space group $P2_1/c$ with one CBZ and half PYZNO molecule in the asymmetric unit. Similar to cocrystal **9**, there is amide dimer homosynthon between CBZ molecules (N1−H1A···O1: 1.97 Å, 2.940(7) Å, 160°) and *anti* amide N−H bonds to *N*-oxide of PYZNO in cocrystal **10** (Figure 10; N1−H1B···O3: 2.10 Å, 3.034(7) Å, 152°). The dibenzazepine group of CBZ is long, and so a spacer molecule is required to fill the voids between homodimers. The helix along the *c*-axis is organized via N1−H1A···O1, N1−H1B···O3, and C−H···O hydrogen bonds (C16−H16···O1, 2.37 Å, 3.081(7) Å, 121°; C17−H17···O1, 2.50 Å, 3.134 (8) Å, 116°).

Cocrystal **10** also falls into strategy 1 wherein the carboxamide homosynthon is retained but the exterior H bond donor (*anti* N−H) is involved in N−H···O⁻ with pyrazine *N,N′*-dioxide. Not surprisingly this cocrystal is isostructural to CBZ·benzoquinone cocrystal. Both benzoquinone and pyrazine *N,N′*-dioxide have similar molecular size and position of H bonding acceptor groups. These crystal structures may be referred to as supramolecular equivalents, or functional group exchange leading to similar crystal packing.[26]

Synthon Trends. Out of 10 crystal structures in this study and 7 from previous work,[14,24] amide−*N*-oxide heterosynthon is present in 12 structures whereas amide dimer homosynthon occurs in 5 structures. In the presence of intramolecular N−H···O H bond, e.g., as in picolinamide−*N*-oxide, the amide dimer is observed.[14] Steric factors favor the homo dimer as noted in carbamazepine cocrystals **9** and **10**; the *anti* NH donor connects dimer aggregates through a CCF spacer. Cocrystal **1** is the only structure in which both amide−*N*-oxide and amide dimer synthons are present. Even though one of the *N*-oxide moieties is free, the amide NH donor does not H bond to it but instead makes a homosynthon. In cocrystal **3**, amide homosynthon is absent but there is a single N−H···O interaction from N−H to the amide carbonyl in a helical motif. This could be due to the 1:0.5 stoichiometry, and it is possible that a 1:1 cocrystal may have a structure with amide−*N*-oxide synthon on both sides, as there is neither steric hindrance nor intramolecular H-bonding complication in **3**. The heterosynthon is also disrupted because of competition from a hydroxyl group, e.g., as in 4-hydroxybenzamide cocrystals **7** and **8**.

(26) Saha, B. K.; Nangia, A. Ethynyl group as a supramolecular halogen and C≡C−H···C≡C trimer synthon in 2,4,6-tris(4-ethynylphenoxy)1,3,5-triazine. *Cryst. Growth Des.* **2007**, *7*, 393−401.

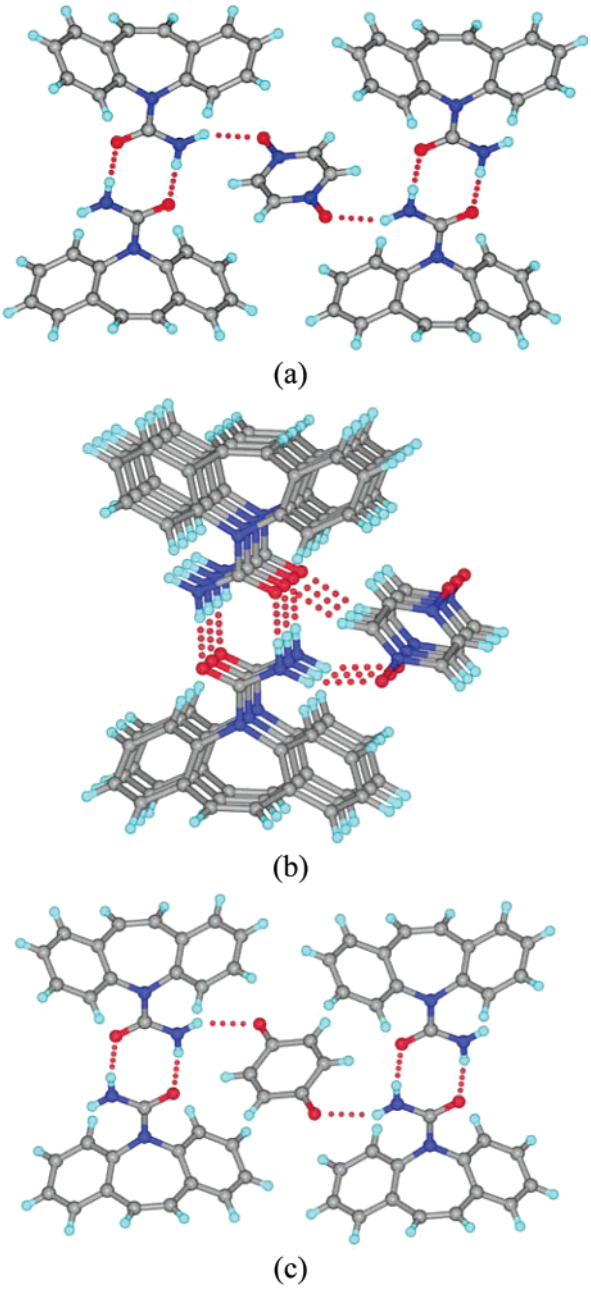

Figure 10. (a) Hydrogen-bonded dimers of CBZ are connected by *anti* N−H···O⁻ H bonds to pyrazine dioxide. (b) Molecular helix viewed down the *c*-axis. Crystal packing in **10** is isostructural to the CBZ·benzoquinone cocrystal, shown in panel c (CSD refcode UNEYOB).

The interfering role of competing functional groups such as H_2O, OH, and NH_2 in amide−*N*-oxide heterosynthon was generalized by a CSD search.[22] Among 41 organic crystal structures of amide and *N*-oxide fragments, there are competing OH, NH functional groups in 14 structures. The amide−*N*-oxide synthon occurs in 11 structures (7 intra- + 4 intermolecular synthons). Of the remaining 27 structures, 21 contain N−H···O⁻ H bond (8 intra- + 13 intermolecular) whereas 5 structures have amide dimer. Details of CSD refcodes in different H bond categories are listed in Table S1.

Pyridine *N*-Oxide Molecules. Oxidation of pyridine nitrogen to *N*-oxide often enhances drug-like behavior to give molecules with good oral bioavailability, pharmacokinetic properties, solubility, and metabolic stability.[27] Affinity at the target receptor or binding site may also increase because of stronger H bonding with the drug molecule. The *N*-oxide is a common route for phase 1 metabolism of drugs containing pyridine moiety, and these metabolites often contribute to drug action. New *N*-oxide drug molecules are popular targets for medicinal chemists. The stronger H bond acceptor strength of *N*-oxide could be exploited to make predictable cocrystals and modified pharmaceuticals with amide-type CCFs.

The hygroscopic nature of several drugs and pharmaceuticals[28] makes it difficult to handle them during formulation and storage. A suitable cocrystal former may be selected such that bonding to the CCF partner satisfies potentially free

(27) (a) Balzarini, J.; Stevens, M.; Clercq, E. D.; Schols D.; Pannecouque, C. Pyridine *N*-oxide Derivatives: Unusual Anti-HIV Compounds with Multiple Mechanisms of Antiviral Action. *J. Antimicrob. Chemother.* **2005**, *55*, 135−138. (b) Anderson, R. F.; Shinde, S.; Hay, M. P.; Gamage, S. A.; Denny, W. A. Radical Properties Governing the Hypoxia-Selective Cytotoxicity of Antitumor 3-Amino-1,2,4-benzotriazine-1,4-dioxides. *Org. Biomol. Chem.* **2005**, *3*, 2167−2174. Tirapazamine (TPZ), a benzotriazine di-*N*-oxide, is the main drug among bioreductive agents and has already demonstrated significant activity in phase II and III clinical trials in combination with radiotherapy and cisplatin based-chemotherapy. (c) Nantermet, P. G.; Burgey, C. S.; Robinson, K. A.; Pellicore, J. M.; Newton, C. L.; Deng, J. Z.; Selnick, H. G.; Lewis, S. D.; Lucas, B. J.; Krueger, J. A.; Miller-Stein, C.; White, R. B.; Wong, B.; McMasters, D. R.; Wallace, A. A.; Lynch, J. J.; Yan, Y.; Chen, Z.; Kuo, L.; Gardell, S. J.; Shafer, J. A.; Vacca, J. P.; Lyle, T. A. P_2 Pyridine *N*-oxide Thrombin Inhibitors: A Novel Peptdomimetic Scaffold. *Bioorg. Med. Chem. Lett.* **2005**, *15*, 2771−2775. (d) Burgey, C. S.; Robinson, K. A.; Lyle, T. A.; Nantermet, P. G.; Selnick, H. G.; Isaacs, R. C.; Dale, L.; Lucas, B. J.; Krueger, J. A.; Singh, R.; Miller-Stein, C.; White, R. B.; Wong, B.; Lyle, E. A.; Stranieri, M. T.; Cook, J. J.; McMasters, D. R.; Pellicore, J. M.; Pal, S.; Wallace, A. A.; Claytond, F. C.; Bohn, D.; Welsh, D. C.; Lynch, J. J.; Jr.; Yan, Y.; Chen, Z.; Kuo, L.; Gardell, S. J.; Shafer, J. A.; Vacca, J. P. Pharmacokinetic Optimization of 3-Amino-6-chloropyrazinone Acetamide Thrombin Inhibitors. Implementation of P_3 Pyridine *N*-oxides to Deliver an Orally Bioavailable Series Containing P_1 *N*-Benzylamides. *Bioorg. Med. Chem. Lett.* **2003**, *13*, 1353−1357. (e) Patel, M. V.; Kolasa, T.; Mortell, K.; Matulenko, M. A.; Hakeem, A. A.; Rohde, J. J.; Nelson, S. L.; Cowart, M. D.; Nakane, M.; Miller, L. N.; Uchic, M. E.; Terranova, M. A.; El-Kouhen, O. F.; Donnelly-Roberts, D. L.; Namovic, M. T.; Hollingsworth, P. R.; Chang, R.; Martino, B. R.; Wetter, J. M.; Marsh, K. C.; Martin, R.; Darbyshire, J. F.; Gintant, G.; Hsieh, G. C.; Moreland, R. B.; Sullivan, J. P.; Brioni, J. D.; Stewart, A. O. Discovery of 3-Methyl-N-(1-oxy-3′,4′,5′,6′-tetrahydro-2′H-[2,4′-bipyridine]-1′-ylmethyl)benzamide (ABT-670), an Orally Bioavailable Dopamine D_4 Agonist for the Treatment of Erectile Dysfunction. *J. Med. Chem.* **2006**, *49*, 7450−7465. (f) Amin, K. M.; Ismail, M. M. F.; Noaman, E.; Solimanb, D. H.; Ammard, Y. A. New Quinoxaline 1,4-di-*N*-oxides. Part 1: Hypoxia-Cytotoxins and Anticancer Agents Derived from Quinoxaline 1,4-Di-*N*-oxides. *Bioorg. Med. Chem.* **2006**, *14*, 6917−6923.

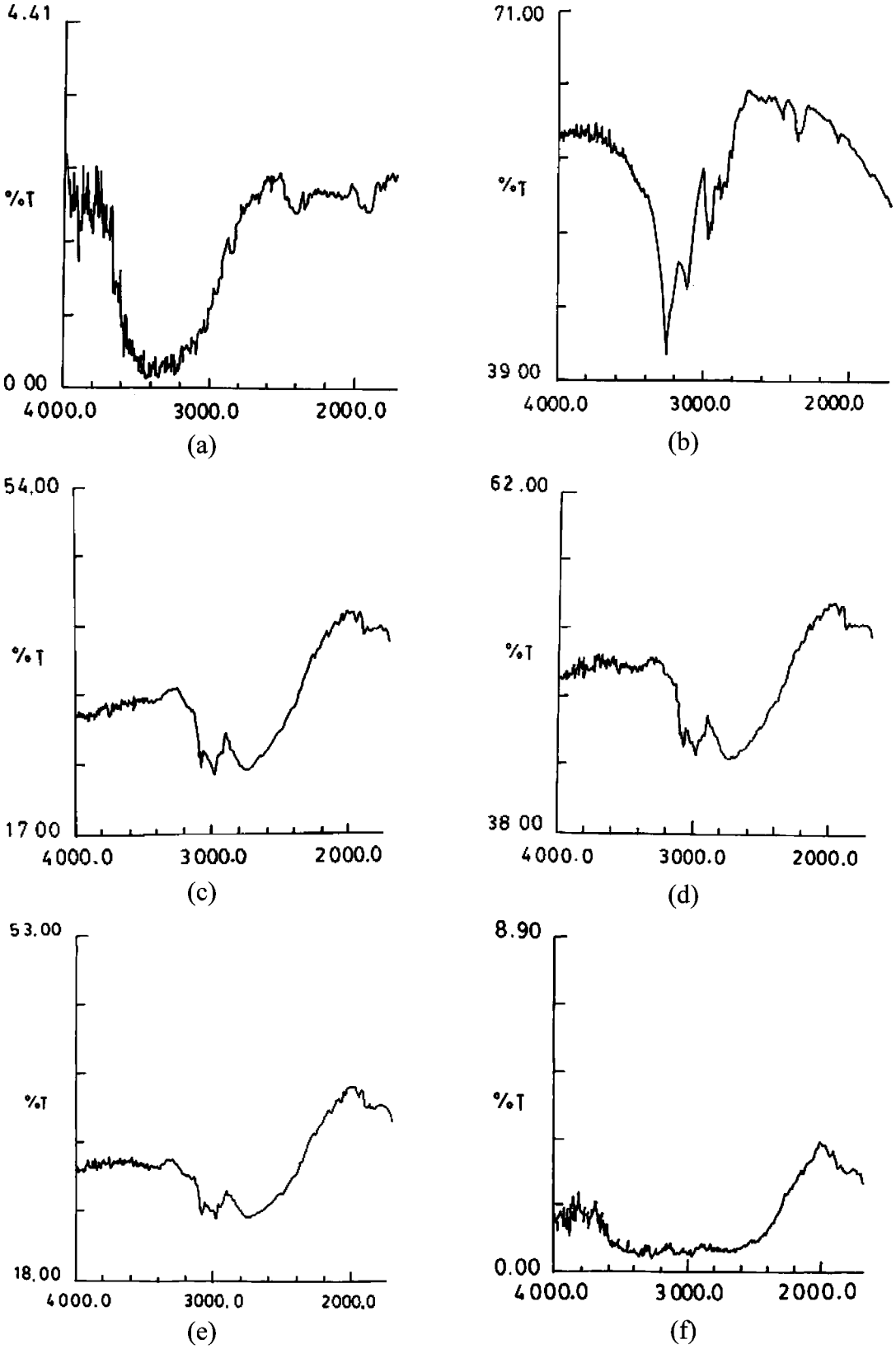

Figure 11. Infrared spectra. (a) 4-Methylpyridine *N*-oxide, the starting material, has a significant amount of moisture based on the broad OH band centered at 3500 cm^{-1}. (b) Barbital has peaks at 3242, 3109, 2961, 2879 cm^{-1}. (c) Cocrystal as prepared; peaks at 3076, 2980, and 2754 cm^{-1}. (d) Cocrystal in open air after 3 days; peaks at 3076, 2980, and 2739 cm^{-1}. (e) Cocrystal in open air after 4 weeks; peaks at 3076, 2976, and 2725 cm^{-1}. (f) Cocrystal in RH 100% after 1 day; the broad band indicates moisture. There is insignificant moisture uptake at 50% RH even after 1 month, but the crystal readily uptakes moisture in saturated water vapor environment. See Figure S11 in the Supporting Information for more plots.

Table 5. Ten Lowest Energy Crystal Structure Frames Computed in Polymorph Predictor Using COMPASS Force Field[a]

	lattice energy/kcal mol^{-1}	density/g cm^{-3}	*a*/Å	*b*/Å	*c*/Å	α/deg	β/deg	γ/deg	*V*/Å^3
			Experimental Crystal Structure (**9**)						
exptl (obs)		1.35	7.284	10.688	14.13	100.25	102.46	109.08	977.7
exptl (min)	−57.573	1.45	7.041	10.613	13.825	101.80	103.65	107.91	911.4
			Predicted Frames of Cocrystal **9**						
1	−57.803	1.45	10.582	13.100	6.920	83.21	72.24	89.50	906.9
2	−57.703	1.46	10.545	13.744	6.854	72.95	72.56	83.85	905.9
3	−57.573	1.45	10.782	13.955	7.041	105.70	110.50	100.10	911.4
4	−55.736	1.46	8.898	7.1522	15.458	68.57	85.45	79.95	901.7
5	−55.248	1.40	7.918	12.092	12.045	64.17	69.06	68.54	938.9
6	−55.087	1.46	8.3682	7.715	14.452	79.52	82.01	83.87	905.4
7	−55.079	1.42	9.448	13.321	8.2156	90.20	105.10	110.70	928.6
8	−55.001	1.42	9.721	12.441	8.328	100.4	105.99	99.48	927.4
9	−54.819	1.46	10.565	7.283	12.481	84.14	70.86	84.82	901.0
10	−54.809	1.41	8.809	10.008	11.382	89.45	81.22	70.63	934.7

[a] The energy difference between predicted frames 1−10 is 3.02 kcal mol^{-1}.

hydrogen bond donors/acceptors sites in the drug molecule. Pyridine *N*-oxides may be co-crystallized with pharmaceutically acceptable carboxamides. An advantage with the amide−*N*-oxide heterosynthon is that H bonding in the cocrystal is sufficiently different from that in the amide dimer, and this should result in unexpected functions and properties of cocrystals. We show proof of concept with 4-methylpyridine *N*-oxide in relation to controlling hydration.

Picoline *N*-oxide is a hygroscopic compound and readily absorbs moisture from the atmosphere during storage and handling.[29] Vacuum drying of PICNO at 110−120 °C showed water absorption bands in its IR spectrum after 3 h. A cocrystal of barbital and picoline *N*-oxide in 1:2 ratio was prepared by grinding in mortar−pestle for 15 min, and the resulting crystalline solid was exposed to different relative humidity conditions (ca. 50% and then 100%) at ambient temperature of ca. 30 °C. IR spectra were recorded at regular intervals (Figure 11), from a few days up to a month, to monitor the increase in intensity of H_2O absorption peaks. These qualitative results show that there is substantial improvement in the hydration stability of a pyridine *N*-oxide by cocrystal formation. A rigorous study on the hydration of 4-picoline *N*-oxide under controlled humidity and temperature conditions is necessary. This approach has utility in pharmaceutical formulation.[30]

Crystal Structure Reproduction. The ab initio crystal structure prediction of an organic molecule[31] is a difficult challenge in pharmaceutical polymorphism given the greater complexity and conformational flexibility of drug molecules. Structure simulation of single component crystal structures ($Z' = 1$) is becoming more manageable, thanks to advancement in computer processing speed and improved software with well-parametrized force fields. Even so, multi-component systems or single-molecule crystal structures having $Z' > 1$ are very difficult or impossible to computationally handle at the present time. We selected carbamazepine·quinoxaline dioxide 1:1 cocrystal (**9**) as a structure prediction (reproduction) test case for the following reasons. (1) It has $Z' = 1$ for each fragment in the observed $P\bar{1}$ crystal structure. Hence computational difficulty is minimal for a two-molecule adduct. (2) This cocrystal is pharmaceutically important as an antiepilepsy drug. (3) The occurrence of amide dimer homosynthon in the observed structure will allow comparison of homo- and heterosynthon hydrogen bonding and the associated molecular packing for each possibility in predicted structure frames. One of the observations that we sought to rationalize by generating several putative structures was to

(28) For example, caffeine, theophylline, paroxetine hydrochloride, chloramphenicol, and carbamazepine exist in hydrated forms. (a) Trask, A.; Motherwell, W. D. S.; Jones, W. Physical stability enhancement of theophylline via cocrystallization. *Int. J. Pharm.* **2006**, *320*, 114−123. (b) Trask, A.; Motherwell, W. D. S.; Jones, W. Pharmaceutical Cocrystallization: Engineering a Remedy for Caffeine Hydration. *Cryst. Growth Des.* **2005**, *5*, 1013−1021. (c) Jayasankar, A.; Somwangthanaroj, A.; Shao, Z. J.; Rodríguez-Hornedo, N. Cocrystal Formation During Cogrinding and Storage is Mediated by Amorphous Phase. *Pharm. Res.* **2006**, *23*, 2381−2392. (d) Matsuo, K.; Matsuoka, M. Solid-State Polymorphic Transition of Theophylline Anhydrate and Humidity Effect. *Cryst. Growth Des.* **2007**, *7*, 411−415.

(29) (a) The Lancaster catalog indicates that picoline *N*-oxide is hygroscopic and should be tightly sealed. When 0.5−1.0 g of the compound was left in an open petri dish for one day at 50% RH conditions at 30 °C (ambient conditions in December in Hyderabad), the solid deliquesced completely. (b) For a recent paper mentioning the hydroscopic nature of this compound, see: Damay, F.; Carretero-Genevrier, A.; Cousson, A.; Van Beek, W.; Rodriguez-Carvajal, J.; Fillaux, F. Synchrotron and Neutron Diffraction Study of 4-Methylpyridine-*N*-oxide at Low Temperature. *Acta Crystallogr.* **2006**, B*62*, 627−633.

(30) Hydrolytic stability of an amide-group-containing API was significantly enhanced in its *N*-oxide cocrystal, unpublished results.

(31) Day, G. M.; Motherwell, W. D. S. Ammon, H.; Boerrigter, S. X. M.; Della Valle, R. G.; Venuta, E.; Dzyabchenko, A.; Dunitz, J. D.; Schweizer, B.; van Eijck, B. P.; Erk, P.; Facelli, J. C.; Bazterra, V. E.; Ferraro, M. B.; Hofmann, D. W. M.; Leusen, F. J. J.; Liang, C.; Pantelides, C. C.; Karamertzanis, P. G.; Price, S. L.; Lewis, T. C.; Nowell, H.; Torrisi, A.; Scheraga, H. A.; Arnautova, Y. A.; Schmidt, M. U.; Verwer, P. A Third Blind Test of Crystal Structure Prediction. *Acta Crystallogr.* **2005**, B*61*, 511−527.

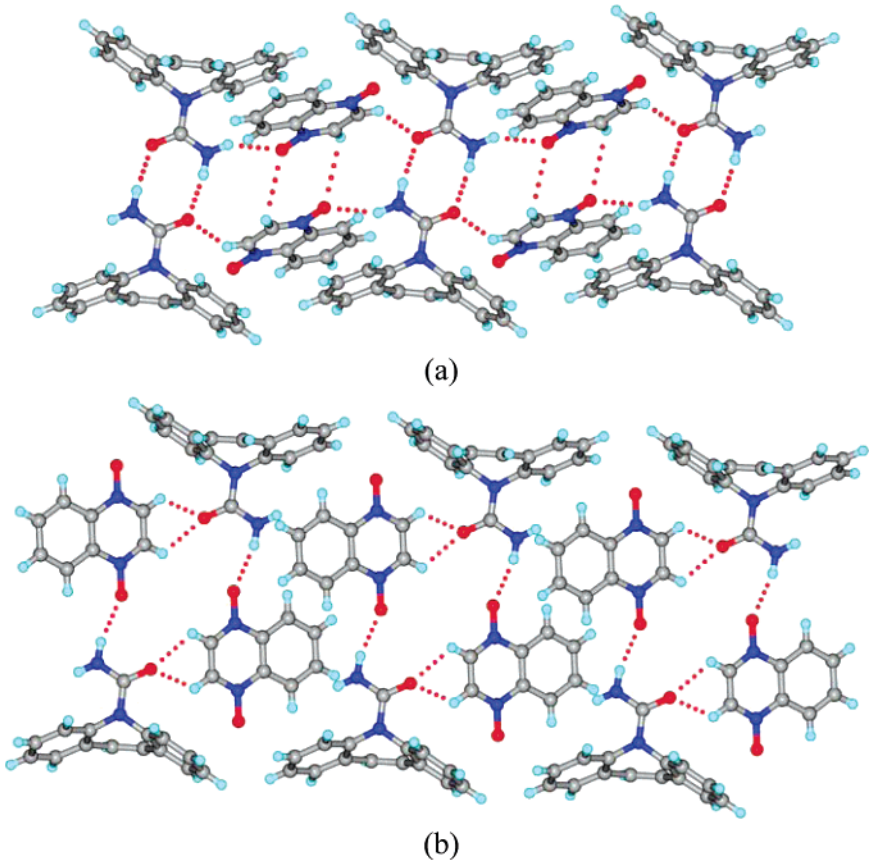

Figure 12. (a) Polymorph Predictor frame 3 of carbamazepine·quinoxaline *N,N′*-dioxide (**9**) to show amide dimer homosynthon of *syn* NH groups and *anti* N−H···O⁻(oxide) hydrogen bond. The third lowest energy predicted structure matches with the observed H bonding and molecular packing shown in Figure 9a. (b) Predicted frame 6 has *syn* (amide)N−H···O⁻(oxide) H bond, but the *anti* NH is free, thereby offering a rationalization for the nonoccurrence of amide−*N*-oxide heterosynthon in CBZ cocrystals.

find out why the stronger amide−*N*-oxide heterosynthon is not common in CBZ cocrystals and instead amide homodimer is present.

Crystal structures were calculated in the Cerius[2] program package using the Polymorph Predictor module and COMPASS force field.[20] Structures were generated keeping the molecular conformation rigid to assess different hydrogen bonding and close packing arrangements. Conformational variations were expected to be minimal for these rigid molecules except torsions in the azepine−amide portion of CBZ.[32] Crystal structures were initially computed only in the observed $P\bar{1}$ space group. A more exhaustive search is currently under way in 10 common space groups. Structure clustering, energy computations, and ranking in increasing lattice energy order were performed next. The energy range for 10 lowest frames is ∼3 kcal mol^{-1}, a value that is comparable to the hydrogen bond energy difference, ΔE_{HB}, between amide dimer homosynthon and amide−*N*-oxide heterosynthon.[14] We therefore expected the 10 lowest energy structures to show homo- and/or heterosynthon hydrogen bonding.

The COSET program (COmpare, SEarch and Topology)[21] allows comparison of structures to identify similar crystal structures within specified tolerances. Establishing isostructurality is important when one has a large list of predicted structures and the aim is to identify predicted structure(s) that match with the experimentally observed structure. Once similar structures are identified, the matching molecular clusters are superposed to visualize the extent of similarity between the two structures. The default size molecule cluster is 15, a central molecule plus its 14 nearest neighbors. Structures are deemed to be the same when all 15 molecules in the coordination shell match nicely. The rms deviation gives a numerical measure of similarity or identity.

Structure prediction frames are listed in Table 5. The unit cell of the third lowest energy frame (referred to as frame 3) matches remarkably well (within 3%) with the observed crystal structure in $P\bar{1}$ space group, and their energies are identical. Match of the observed crystal structure with any one of the low-energy frames (typically frames 1−5, <1 kcal mol^{-1} above the global minimum) is considered to be a good result in the current day.[33] N−H···O and C−H···O hydrogen bonds between carbamazepine and quinoxaline dioxide molecules are identical in the experimental and simulated frame 3 (Figure 12). The overlay of 15 nearest-neighbor

(32) Cabera, A. J. C; Day, G. M.; Motherwell, W. D. S.; Jones, W. Amide Pyramidalization in Carbamazeoine: A Flexibility Problem in Crystal Structure Prediction? *Cryst. Growth Des.* **2006**, *6*, 1858−1866.

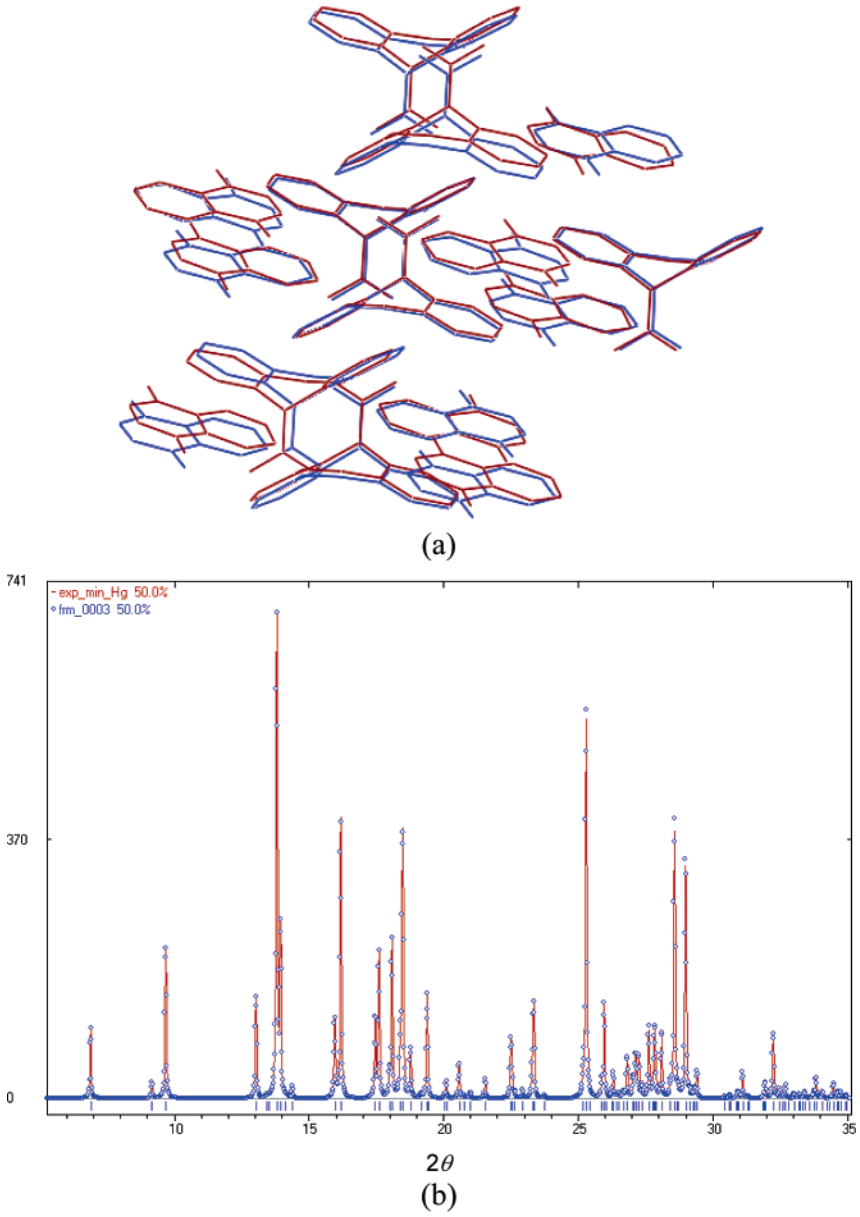

Figure 13. Overlay of 15 nearest neighbor molecules of experimental carbamazepine−quinoxaline *N,N′*-dioxide cocrystal and simulated frame 3. The rms deviation is 0.335 Å, indicating identity between these two structures. (b) Overlay of powder XRD profile of experimental minimized (red) and predicted structure 3 (blue) show excellent match in peak position and intensity.

molecules shows excellent superposition, rms deviation of 0.335, and good overlay in the position and intensity of powder X-ray diffraction peaks (Figure 13). On the other hand, lower energy frames 1 and 2 do not match well in terms of triclinic unit cell angles (though the distances are comparable, Table 4). Predicted structures in the lowest and next higher energy frames 1 and 2 have the amide homodimer. However, it was not possible to overlay molecules in these energetically favored predicted structures with the experimental crystal structure because of gross differences in molecular arrangement. Frame 6, the sixth lowest energy predicted structure, contains amide−*N*-oxide *syn* N−H···O$^-$ hydrogen bond (Figure 12). Closer examination of this structure suggested that a reason for the nonoccurrence of amide−*N*-oxide heterosynthon in CBZ cocrystals is steric. The *anti* NH donor surprisingly is not H bonded to the available *N*-oxide acceptor in computed structure frame 6 because the dibenzazepine ring of this rigid, butterfly-shaped molecule, which overhangs just above the *anti* NH donor, blocks close approach of potential hydrogen bond acceptors. There is however a long, bent

(33) (a) Roy, S.; Banerjee, R.; Nangia, A.; Kruger, G. J. Conformational, concomitant polymorphs of 4,4-diphenyl-2,5-cyclohexadienone. Conformation and lattice energy compensation in kinetic and thermodynamic forms. *Chem. Eur. J.* **2006**, *12*, 3777−3788. (b) Lewis, T. C.; Tocher, D. A.; Price, S. L. Investigating Unused Hydrogen Bond Acceptors Using Known and Hypothetical Crystal Polymorphism. *Cryst. Growth Des.* **2005**, *5*, 983−993.

Table 6. Hydrogen Bonding in Ten Lowest Energy Structures of Carbamazepine·Quinoxaline Dioxide Cocrystal (**9**) Predicted in $P\bar{1}$ Space Group[a]

hydrogen-bonding synthon	frames
amide−amide homosynthon, *anti* N−H···O$^-$ H bond	1, 2, 3, 7, 8
amide−*N*-oxide heterosynthon, no amide homosynthon	6
amide homosynthon, no *anti* N−H···O$^-$ H bond	5, 10
no amide homosynthon, no N−H···O$^-$ H bond	4, 9

[a] These frames may be viewed in Mercury[22] (.cif format), Supporting Information.

(CBZamide)N−H···π(QUINOphenyl) interaction (3.08 Å, 124°). Among 10 lowest energy frames in $P\bar{1}$ space group, five structures contain amide homodimer and one structure has amide−*N*-oxide heterosynthon (Table 6).

Conclusions

The amide−*N*-oxide heterosynthon offers a crystal engineering strategy to construct cocrystals of both carboxamide and pyridine *N*-oxide type molecules with complementary CCFs. We demonstrated carbamazepine, barbiturate, and saccharin as pharmaceutical examples of cocrystals. The probability of heterosynthon formation is good based on the strongest donor (CONH) hydrogen bonding to the strongest acceptor (N$^+$−O$^-$) in the system.[34] Hydrogen bonding in heterosynthon-mediated cocrystals is significantly different from that in the constituent molecules which have homosynthon H bonding (i.e., category 2 cocrystals),[25] and hence the physical and chemical properties of cocrystals are expected to be different from those of the pure components. For example, 4-picoline *N*-oxide·barbital cocrystal is hydrolytically stable compared to immediate hydration of pure picoline *N*-oxide. Drug molecules containing the *N*-oxide moiety may be co-crystallized with GRAS amides or additives (generally regarded as safe, e.g., acetamide, butyramide, 3,5-dinitrobenzamide).[35] Crystal structure prediction of binary cocrystals is a very recent development.[36] Full structure prediction results on carbamazepine·quinoxaline *N*,*N*′-dioxide cocrystal (**9**) will be detailed in a future article.

Acknowledgment. We thank DST (SR/S5/OC-02/2002 and SR/S1/RFOC-01/2007) and CSIR (01(2079)/06/EMR-II) for funding. UGC and CSIR provided fellowship to N.J.B. and L.S.R. DST (IRPHA) funds the CCD X-ray diffractometer, and the CMSD-HPC facility is supported by DST-UPE. UGC is thanked for the UPE program.

Supporting Information Available: ORTEPs of molecular fragments, IR plots, CSD refcodes, crystal structures **1**−**10** (.cif), and predicted frames of cocrystal **9** (.cif). This material is available via the Internet at http://pubs.acs.org.

MP070014C

(34) Etter, M. C. Encoding and Decoding Hydrogen-Bond Patterns of Organic Compounds. *Acc. Chem. Res.* **1990**, *23*, 120−126.
(35) List of GRAS chemicals is available at http://www.cfsan.fda.gov/~dms/eafus.html.
(36) Cruz Cabeza, A. J.; Day, G. M.; Motherwell, W. D. S.; Jones, W. Prediction and Observation of Isostructurality Induced by Solvent Incorporation in Multicomponent Crystals. *J. Am. Chem. Soc.* **2006**, *128*, 14466−14467.